

Prediction and understanding of experimental synthesized IRMOF-14 and its analogues (*M*-IRMOF-14, *M*=cadmium, alkaline earth metals) on the electronic structure, structural stability, chemical bonding, and optical properties

Supporting Information

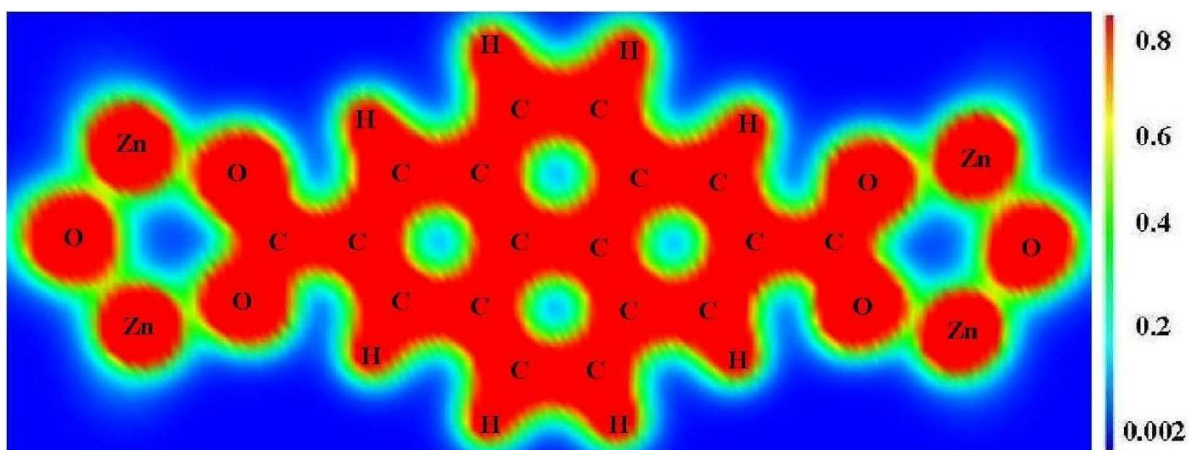
Li-Ming Yang*[†], Ponniah Ravindran[‡], Ponniah Vajeeston[‡], and Mats Tilset*[†]

[†]*Center of Theoretical and Computational Chemistry, Department of Chemistry, University of Oslo, P.O.Box 1033 Blindern, N-0315 Oslo, Norway,* [‡]*Center for Materials Science and Nanotechnology, Department of Chemistry, University of Oslo, P.O.Box 1033 Blindern, N-0315 Oslo, Norway*

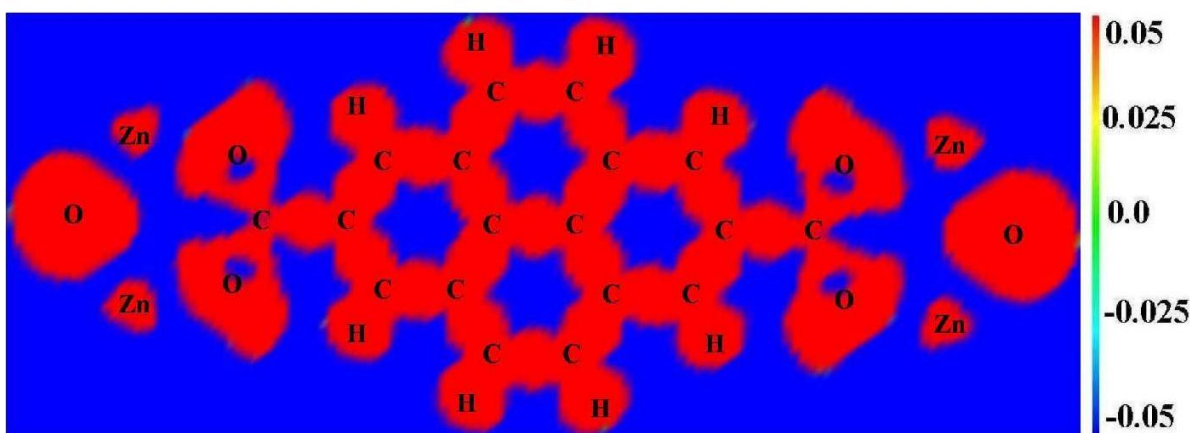
(E-mail of corresponding authors: mats.tilset@kjemi.uio.no and l.m.yang@kjemi.uio.no.; Fax: +47 22855441;)

Page 2, **Fig. S1.** Calculated charge density, charge transfer, and ELF plots for Zn-IRMOF-14
Page 3, **Fig. S2.** Calculated charge density, charge transfer, and ELF plots for Cd-IRMOF-14
Page 4, **Fig. S3.** Calculated charge density, charge transfer, and ELF plots for Be-IRMOF-14
Page 5, **Fig. S4.** Calculated charge density, charge transfer, and ELF plots for Mg-IRMOF-14
Page 6, **Fig. S5.** Calculated charge density, charge transfer, and ELF plots for Ca-IRMOF-14
Page 7, **Fig. S6.** Calculated charge density, charge transfer, and ELF plots for Sr-IRMOF-14
Page 8, **Fig. S7.** Calculated charge density, charge transfer, and ELF plots for Ba-IRMOF-14
Page 9, **Fig. S8.** Calculated TDOS and PDOS for Cd-IRMOF-14
Page 10, **Fig. S9.** Calculated TDOS and PDOS for Be-IRMOF-14
Page 11, **Fig. S10.** Calculated TDOS and PDOS for Mg-IRMOF-14
Page 12, **Fig. S11.** Calculated TDOS and PDOS for Ca-IRMOF-14
Page 13, **Fig. S12.** Calculated TDOS and PDOS for Sr-IRMOF-14
Page 14, **Fig. S13.** Calculated TDOS and PDOS for Ba-IRMOF-14

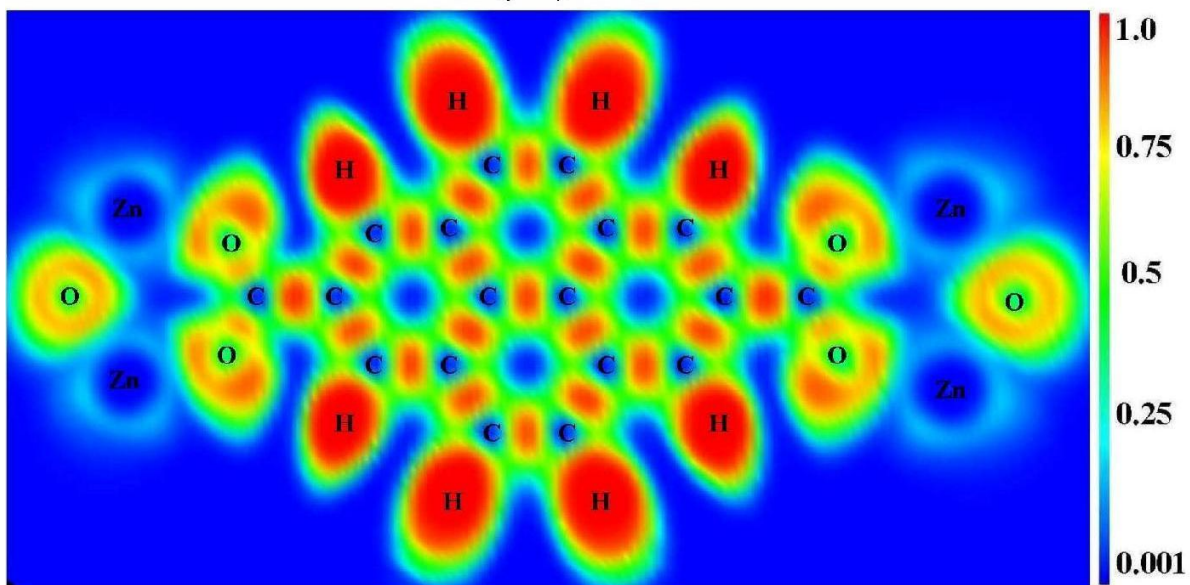
Page 15, **Fig. S14.** Calculated optical properties for Cd-IRMOF-14
Page 16, **Fig. S15.** The electronic band structure of Cd-IRMOF-14
Page 17, **Fig. S16.** Calculated optical properties for Be-IRMOF-14
Page 18, **Fig. S17.** The electronic band structure of Be-IRMOF-14
Page 19, **Fig. S18.** Calculated optical properties for Mg-IRMOF-14
Page 20, **Fig. S19.** The electronic band structure of Mg-IRMOF-14
Page 21, **Fig. S20.** Calculated optical properties for Ca-IRMOF-14
Page 22, **Fig. S21.** The electronic band structure of Ca-IRMOF-14
Page 23, **Fig. S22.** Calculated optical properties for Sr-IRMOF-14
Page 24, **Fig. S23.** The electronic band structure of Sr-IRMOF-14
Page 25, **Fig. S24.** Calculated optical properties for Ba-IRMOF-14
Page 26, **Fig. S25.** The electronic band structure of Ba-IRMOF-14
Page 27, **Table S1.** Mulliken effective charges (MEC), bond overlap populations (BOP), and Bader charges (BC) for *M*-IRMOF-14 (*M* = Zr, Cd, Be, Mg, Ca, Sr, Ba)



(a)

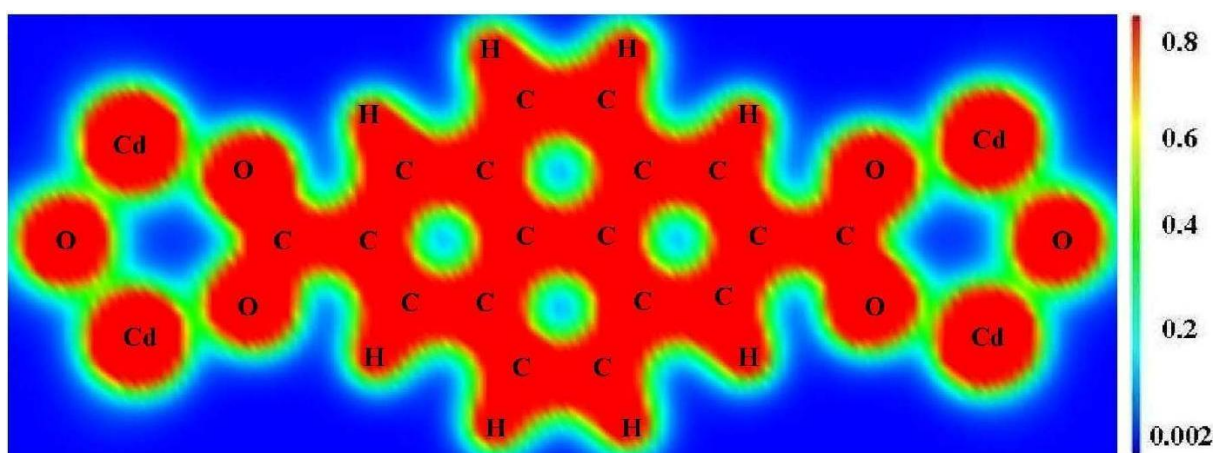


(b)

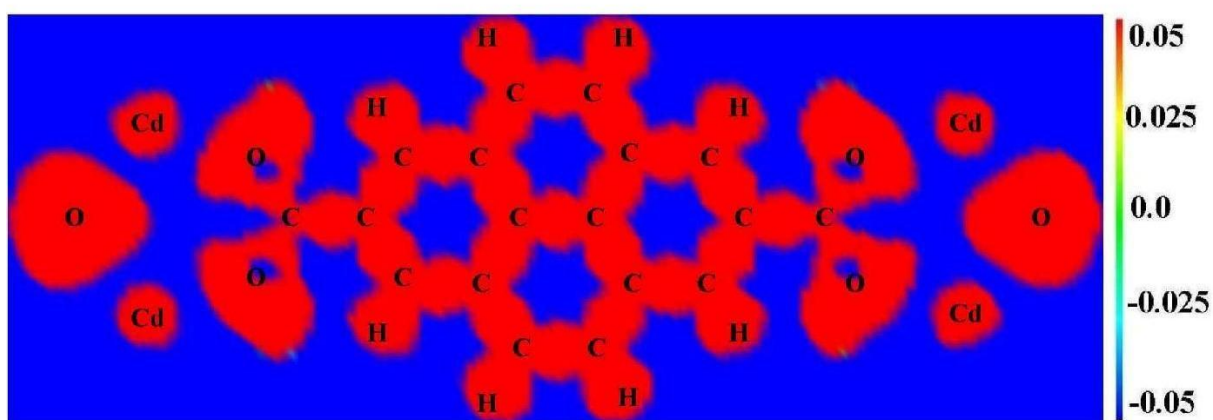


(c)

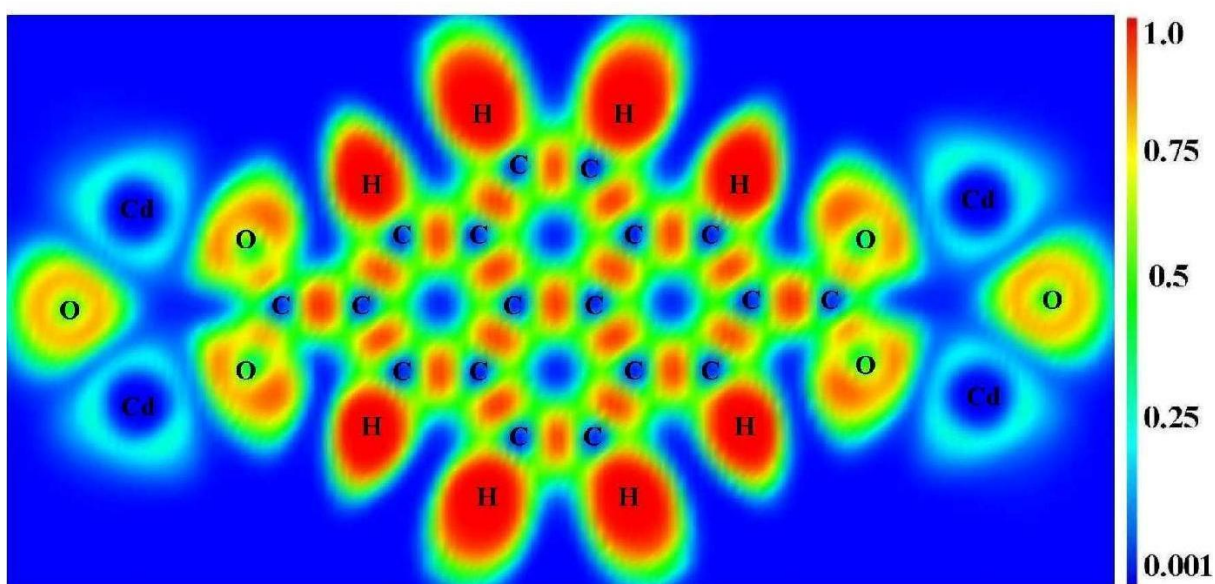
Figure S1. Calculated charge density (a), charge transfer (b), and electron localization function (c) plots for Zn-IRMOF-14 in the (110) plane.



(a)

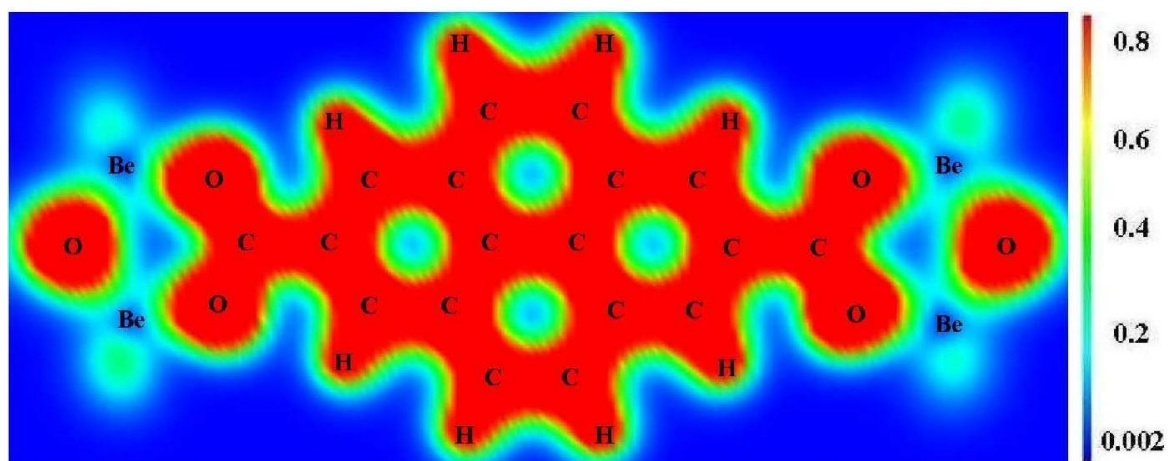


(b)

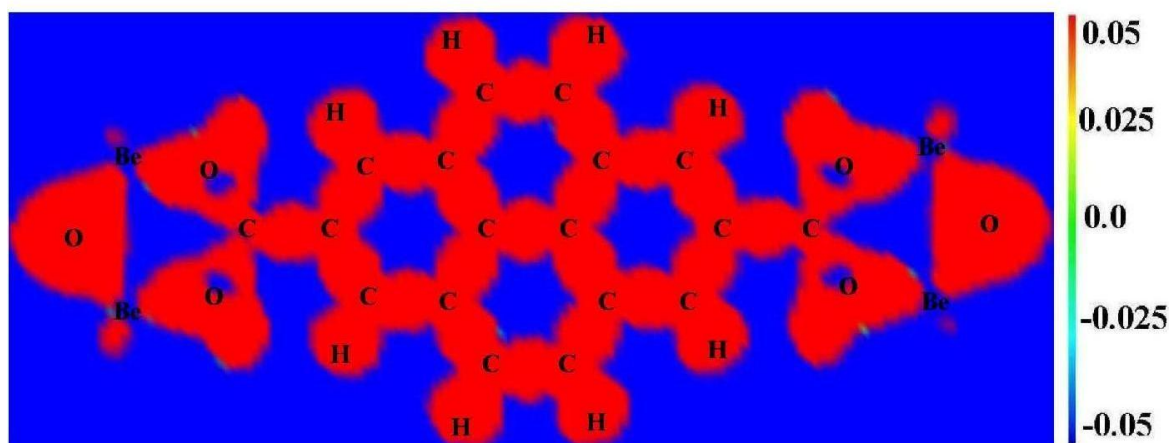


(c)

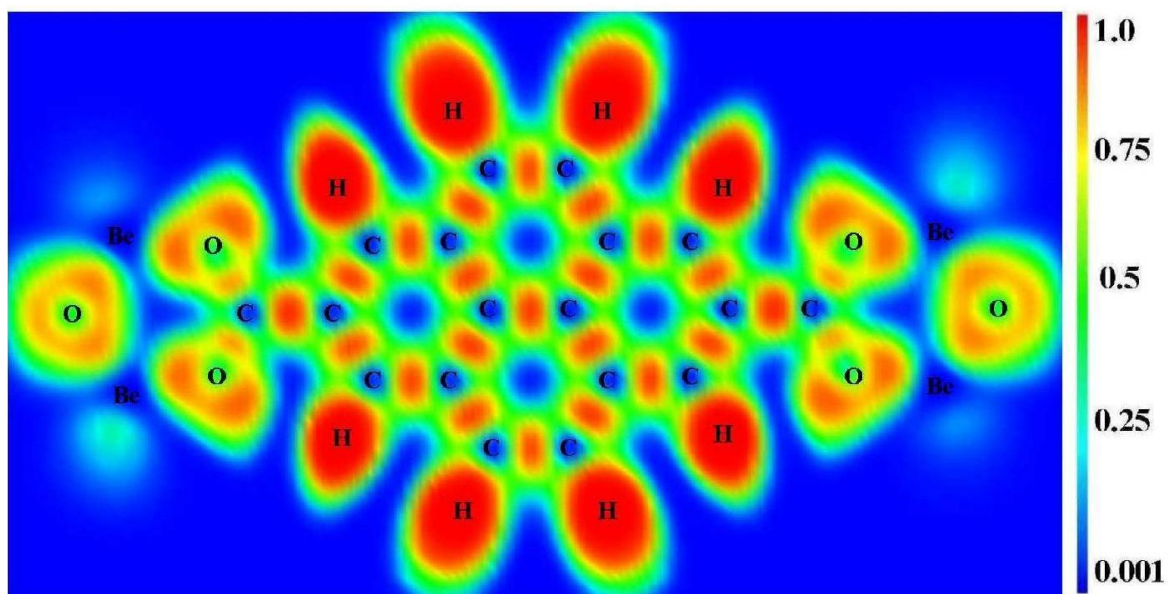
Figure S2. Calculated charge density (a), charge transfer (b), and electron localization function (c) plots for Cd-IRMOF-14 in the (110) plane.



(a)

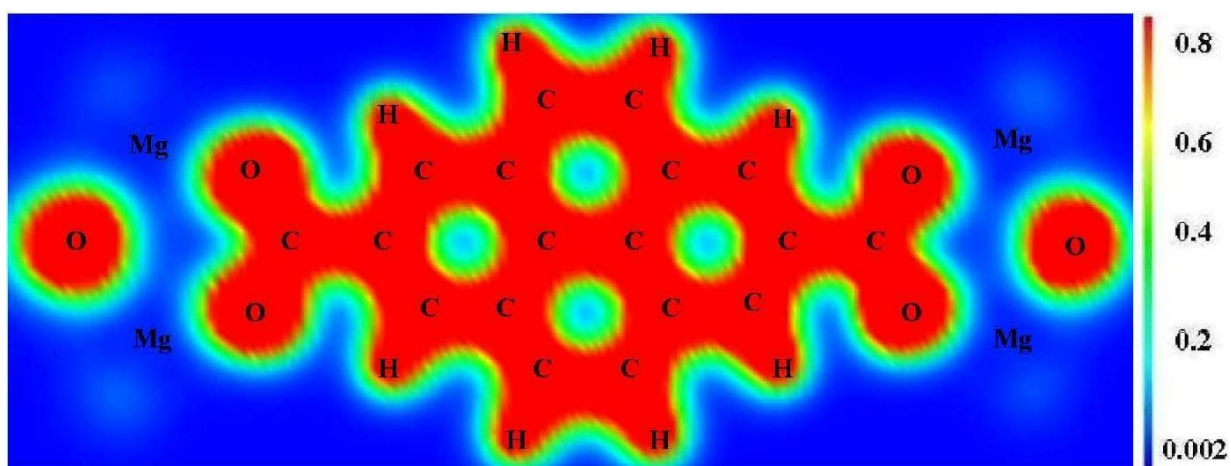


(b)

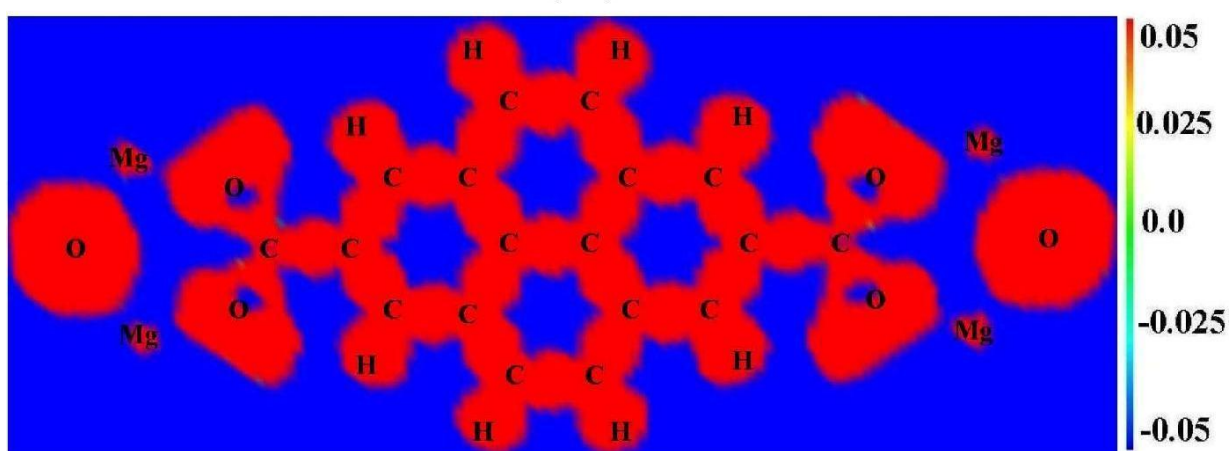


(c)

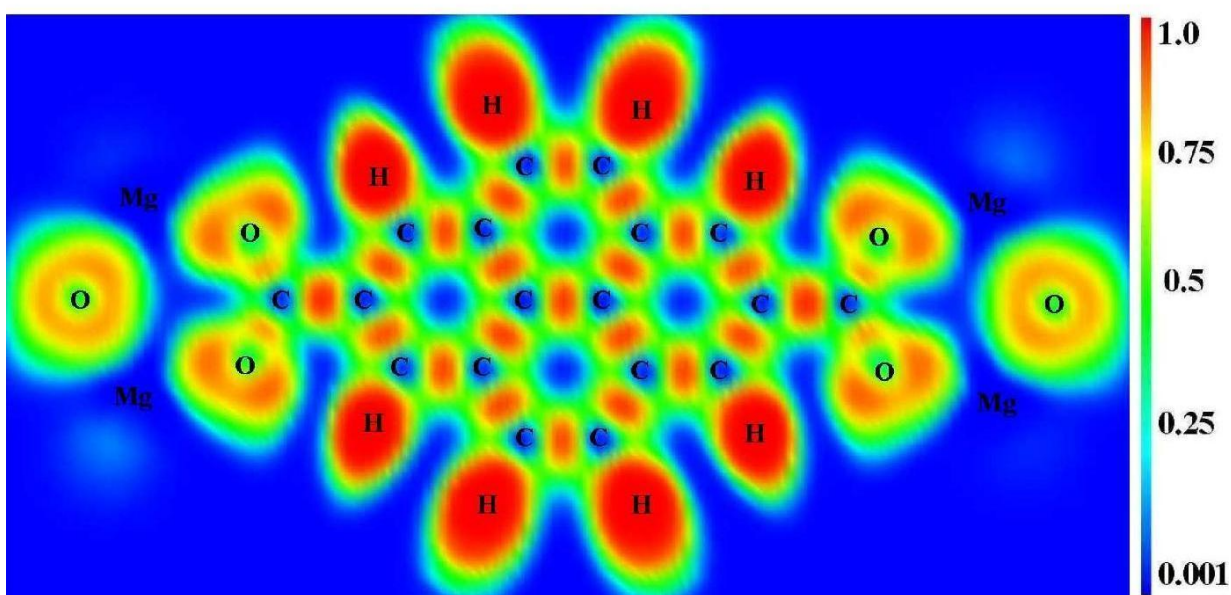
Figure S3. Calculated charge density (a), charge transfer (b), and electron localization function (c) plots for Be-IRMOF-14 in the (110) plane.



(a)

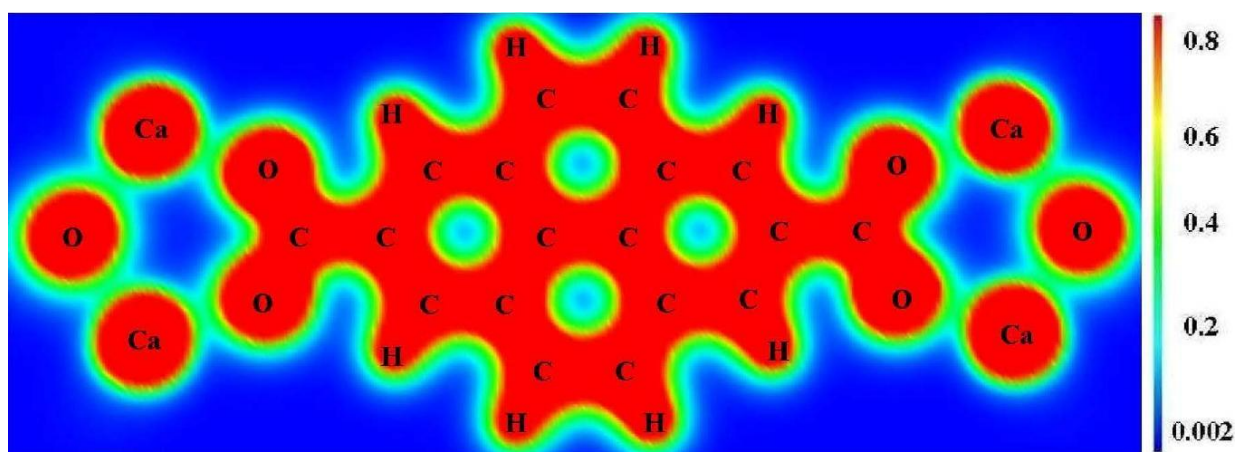


(b)

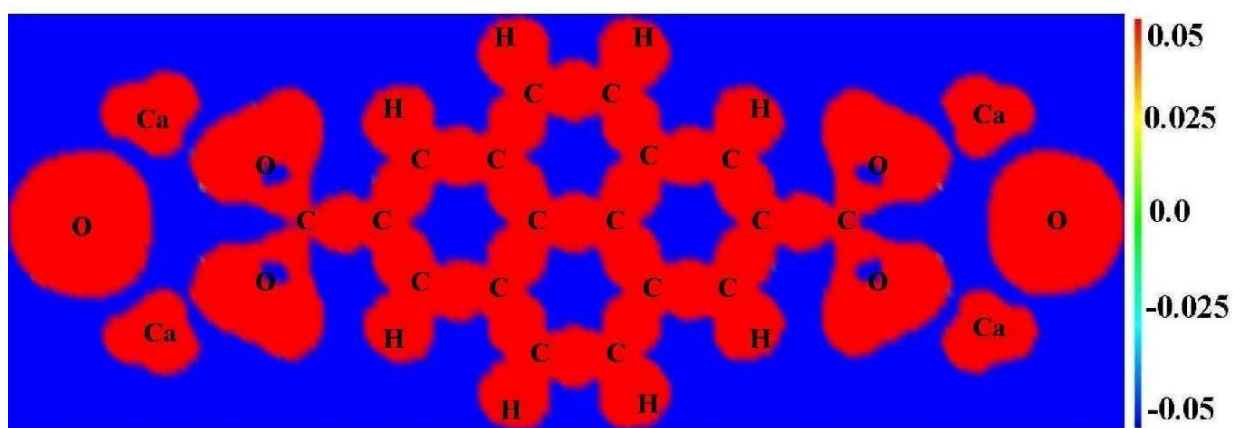


(c)

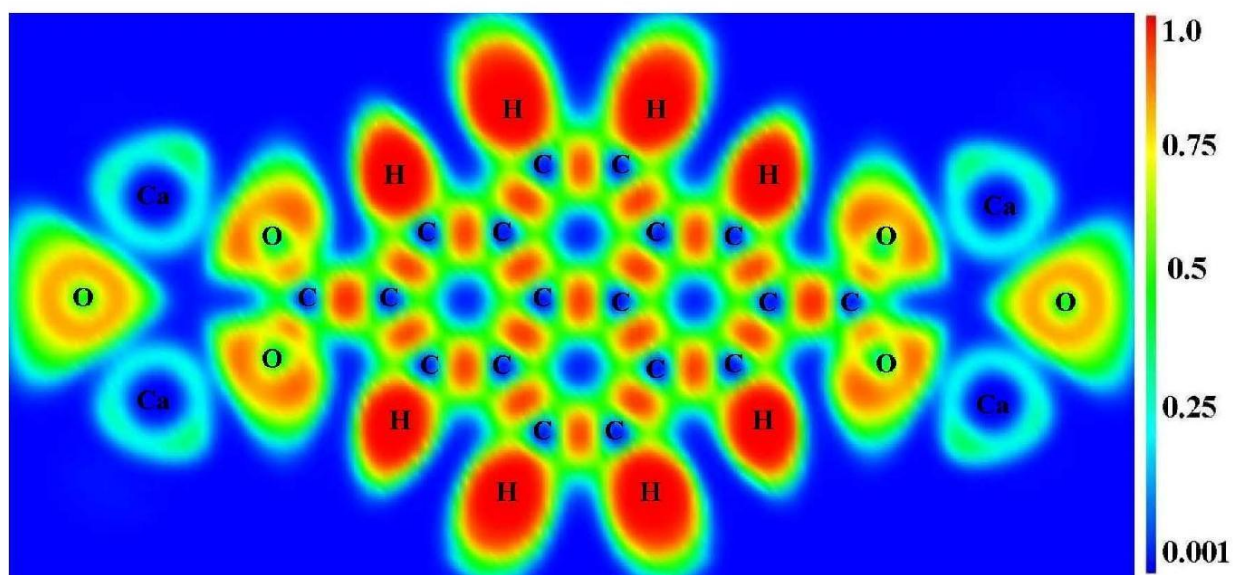
Figure S4. Calculated charge density (a), charge transfer (b), and electron localization function (c) plots for Mg-IRMOF-14 in the (110) plane.



(a)

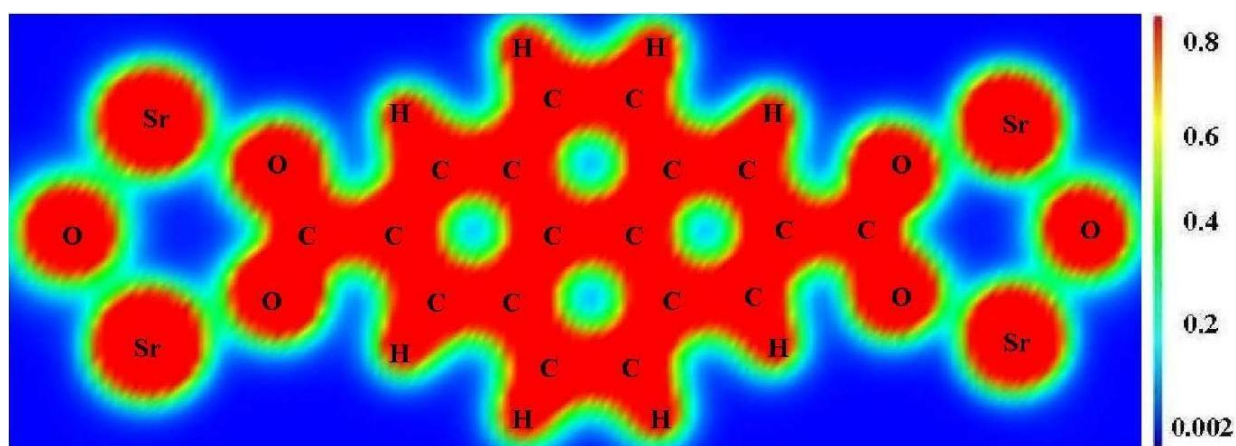


(b)

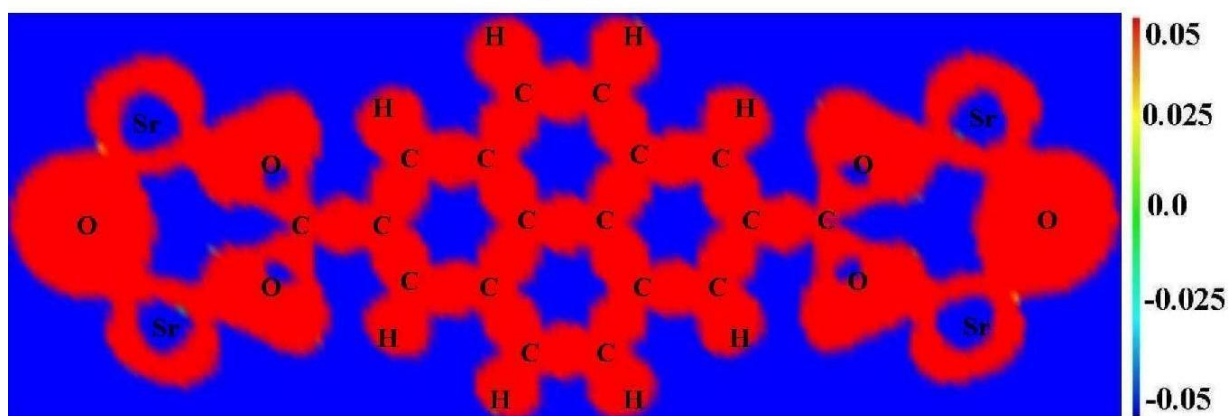


(c)

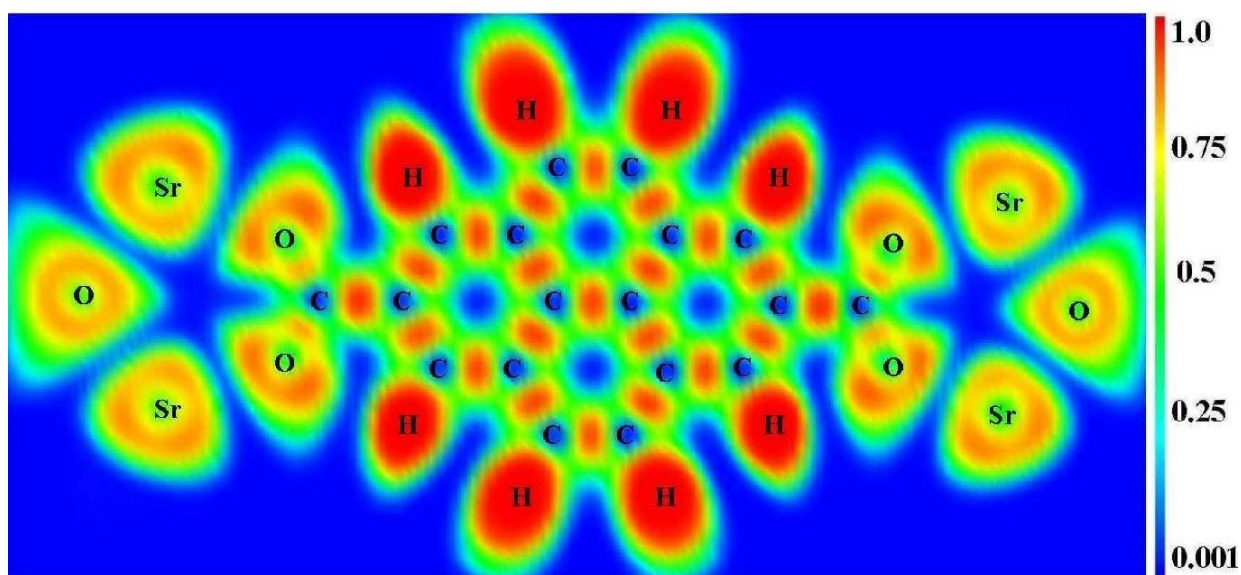
Figure S5. Calculated charge density (a), charge transfer (b), and electron localization function (c) plots for Ca-IRMOF-14 in the (110) plane.



(a)

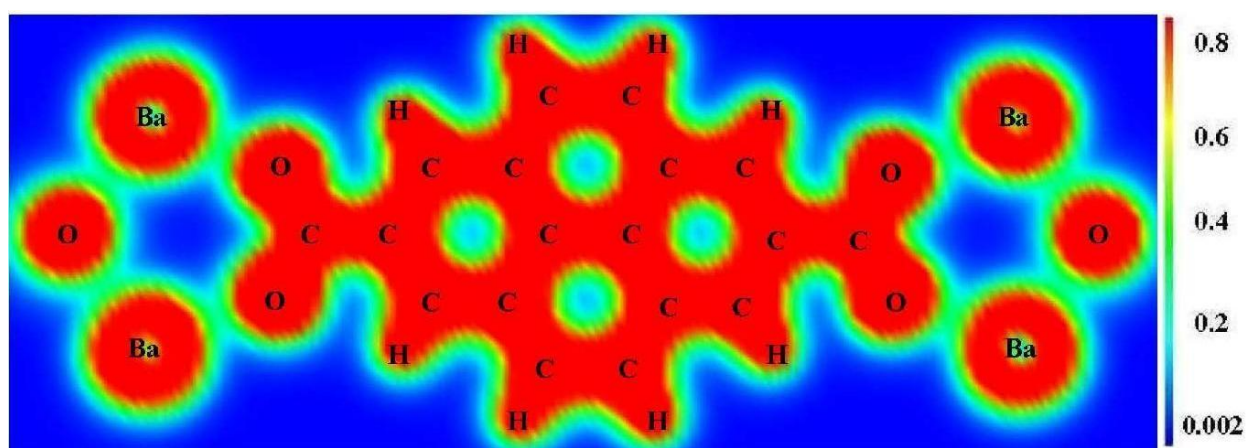


(b)

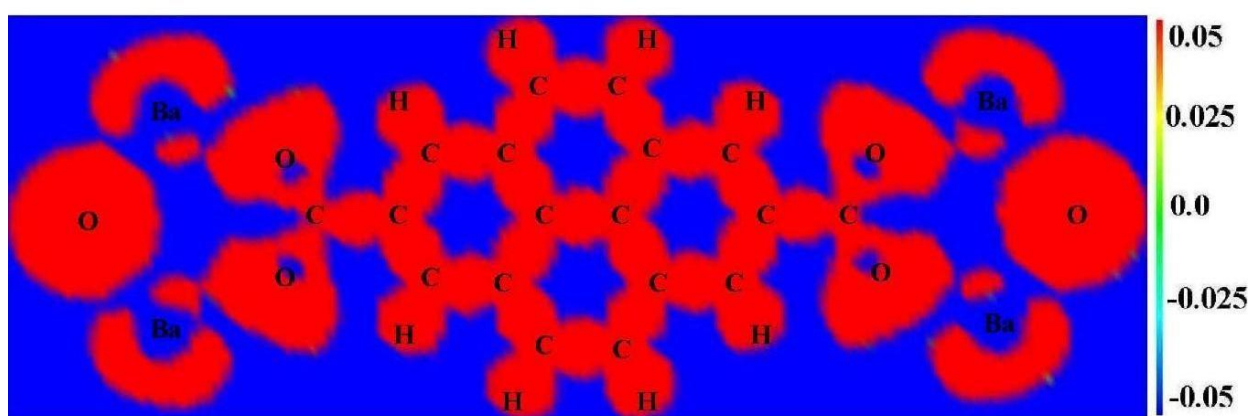


(c)

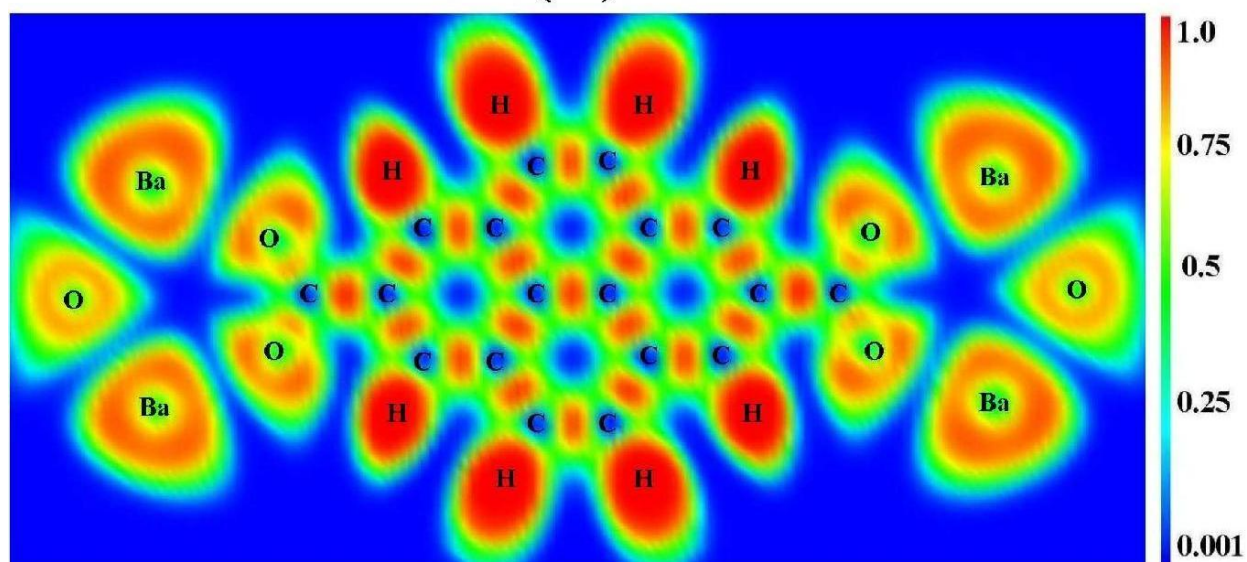
Figure S6. Calculated charge density (a), charge transfer (b), and electron localization function (c) plots for Sr-IRMOF-14 in the (110) plane.



(a)



(b)



(c)

Figure S7. Calculated charge density (a), charge transfer (b), and electron localization function (c) plots for Ba-IRMOF-14 in the (110) plane.

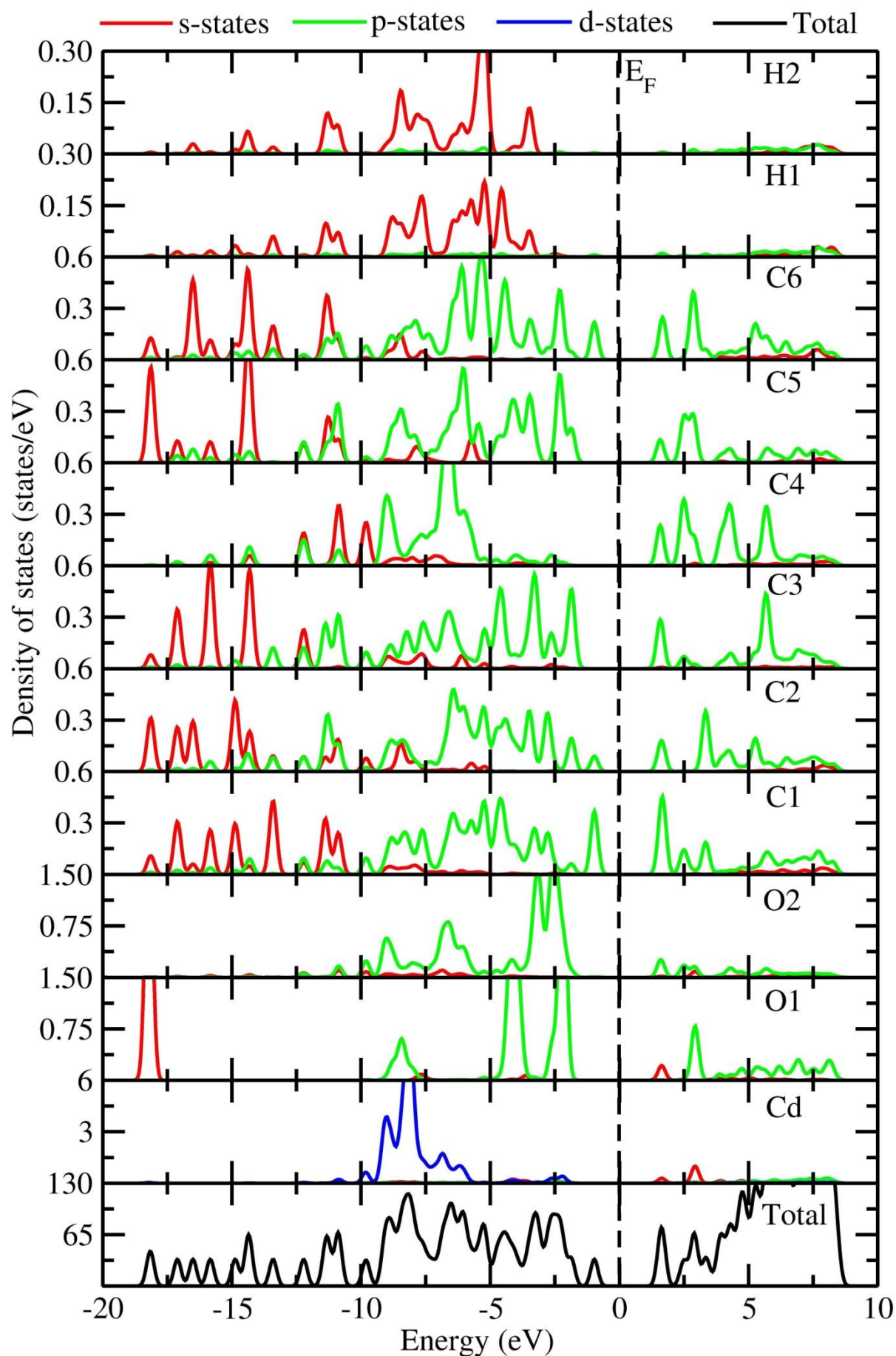


Figure S8. The calculated total density of states (TDOS) and partial density of states (PDOS) for Cd-IRMOF-14 in the cubic $Fm-3m$ symmetry (no. 225)

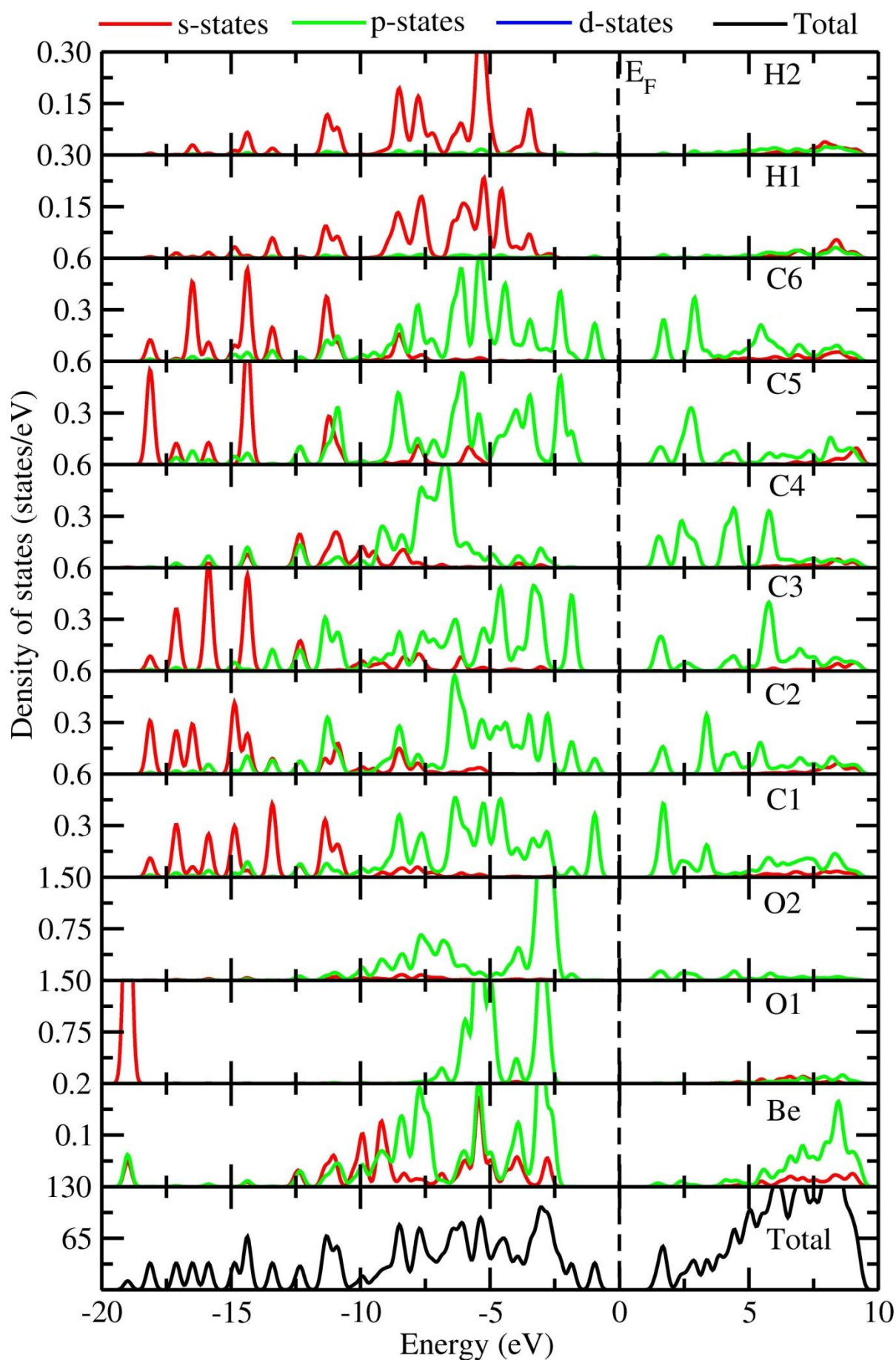


Figure S9. The calculated total density of states (TDOS) and partial density of states (PDOS) for Be-IRMOF-14 in the cubic $Fm-3m$ symmetry (no. 225)

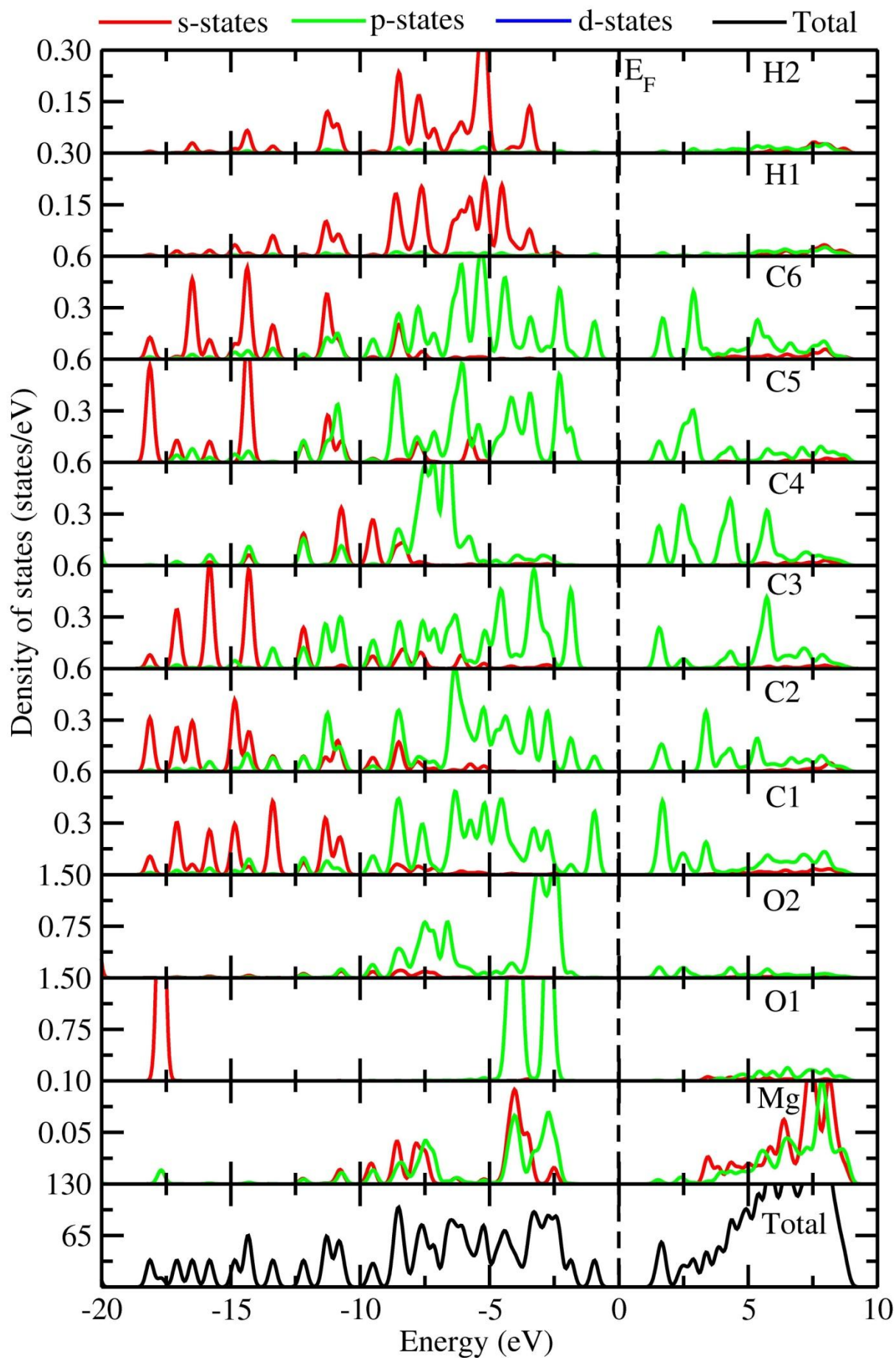


Figure S10. The calculated total density of states (TDOS) and partial density of states (PDOS) for Mg-IRMOF-14 in the cubic $Fm-3m$ symmetry (no. 225)

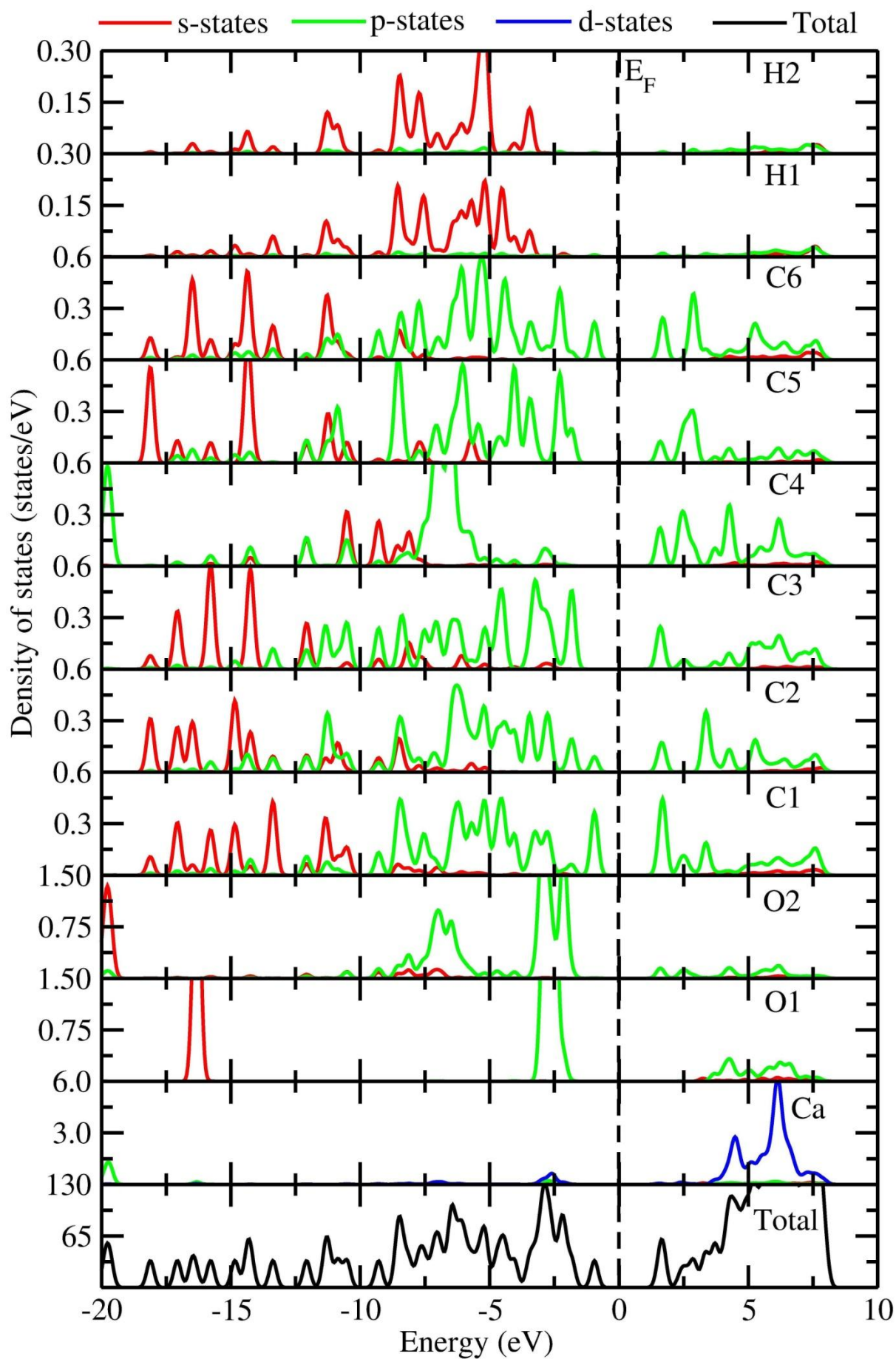


Figure S11. The calculated total density of states (TDOS) and partial density of states (PDOS) for Ca-IRMOF-14 in the cubic $Fm-3m$ symmetry (no. 225)

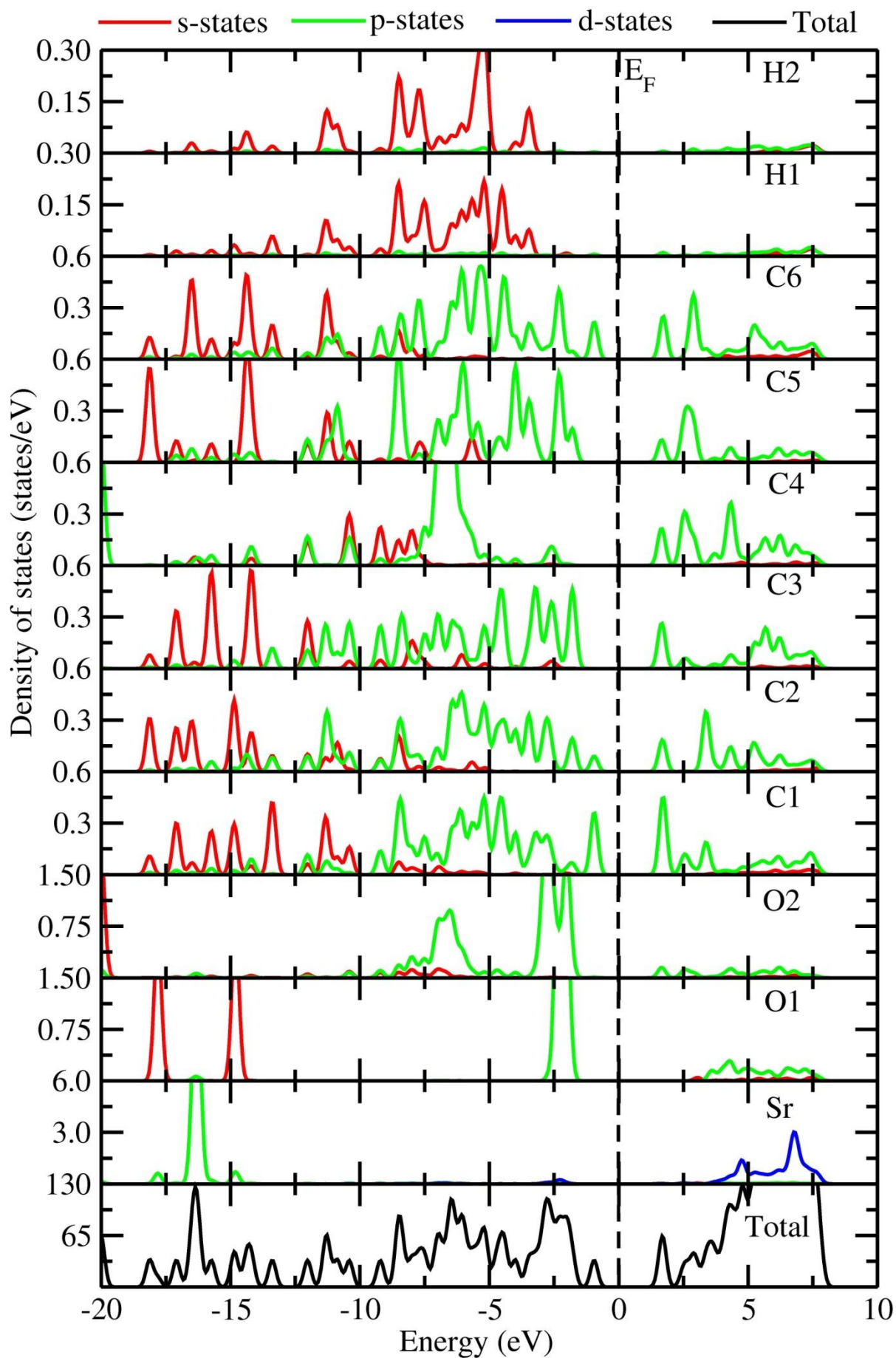


Figure S12. The calculated total density of states (TDOS) and partial density of states (PDOS) for Sr-IRMOF-14 in the cubic $Fm-3m$ symmetry (no. 225)

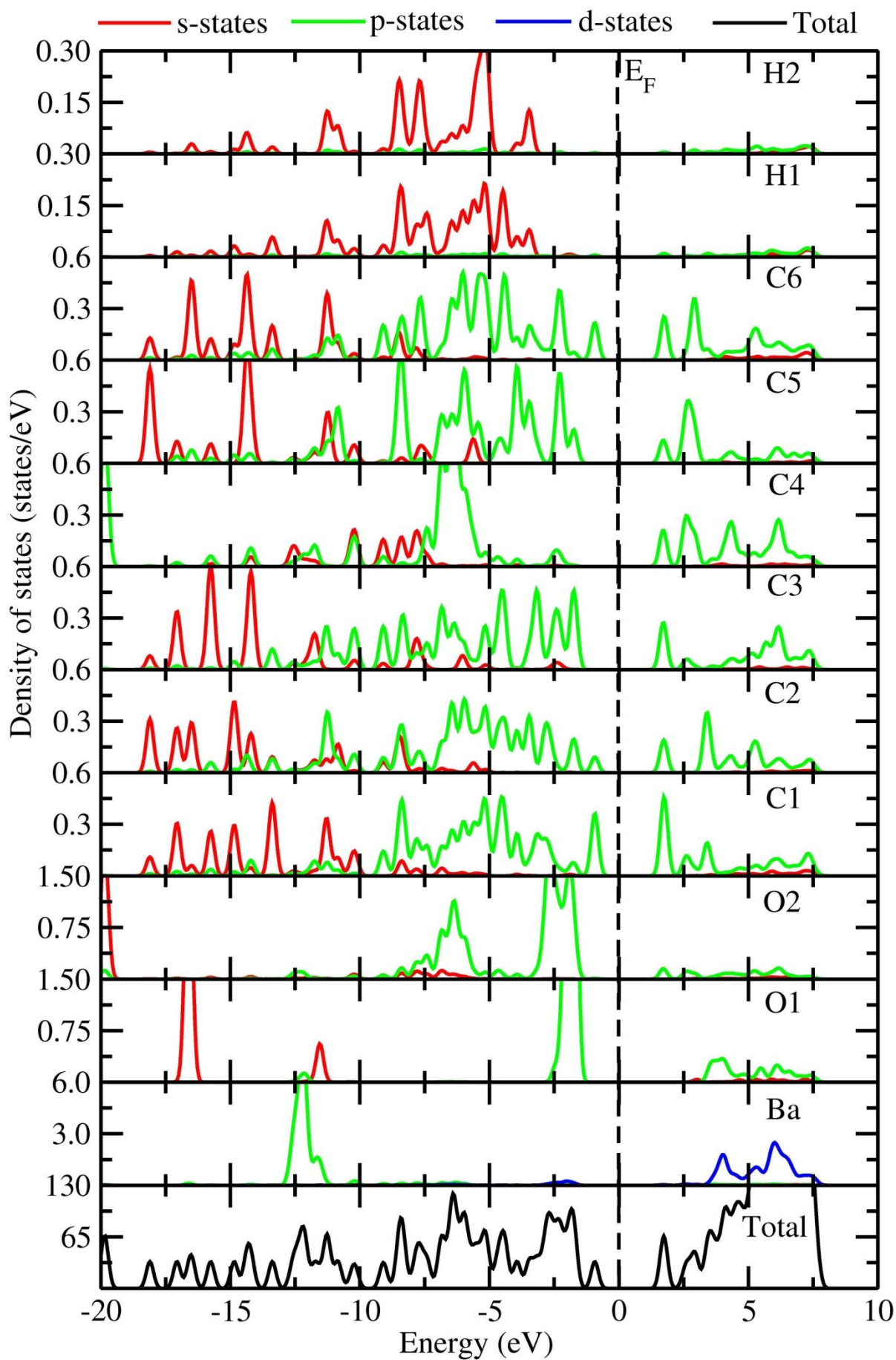


Figure S13. The calculated total density of states (TDOS) and partial density of states (PDOS) for Ba-IRMOF-14 in the cubic $Fm-3m$ symmetry (no. 225)

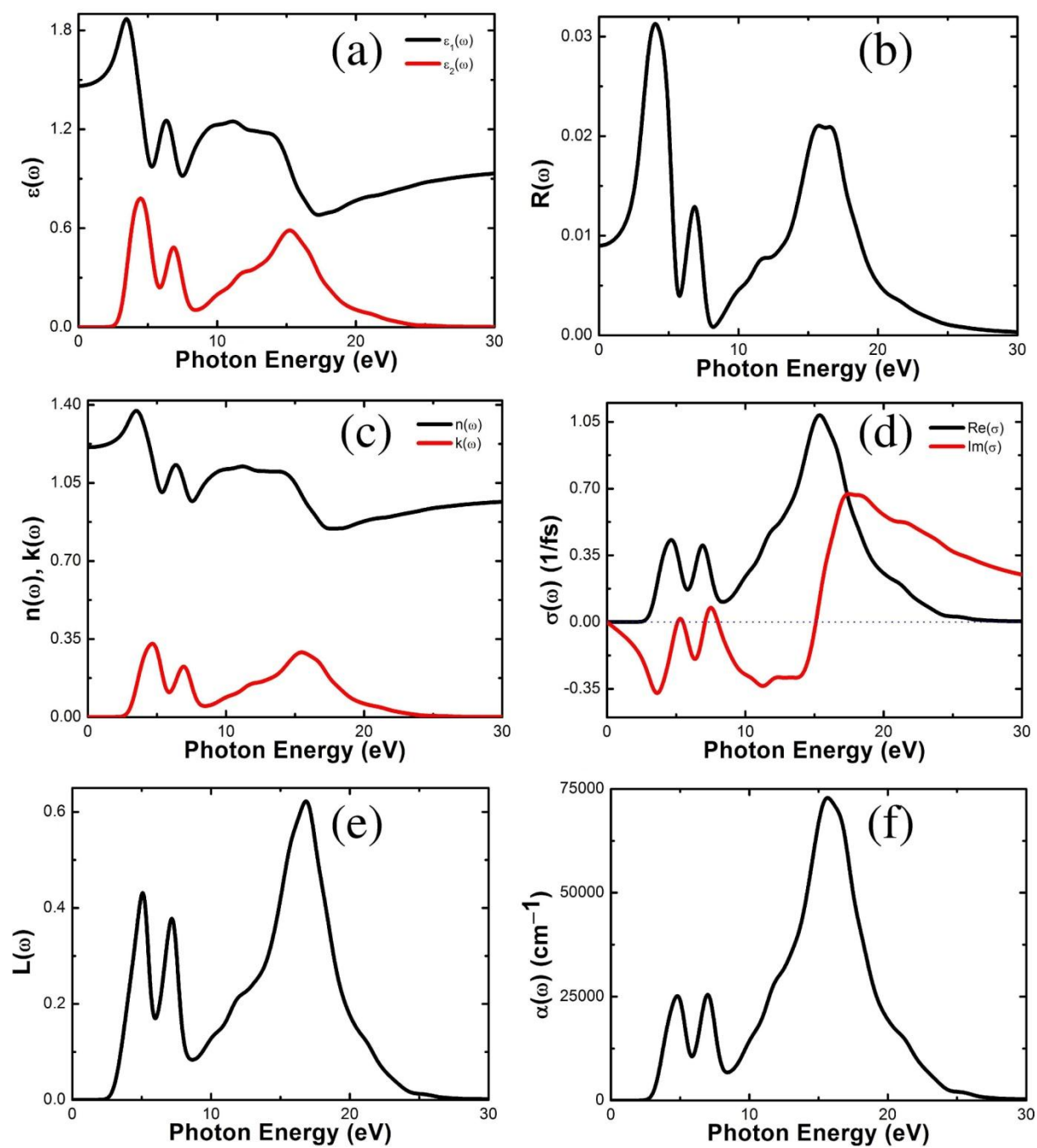


Figure S14. Calculated optical properties for Cd-IRMOF-14: (a) dielectric function $\epsilon(\omega)$, (b) reflectivity $R(\omega)$, (c) refractive index $n(\omega)$; extinction coefficient $k(\omega)$, (d) optical conductivity $\sigma(\omega)$, (e) energy loss function $L(\omega)$, (f) absorption $\alpha(\omega)$.

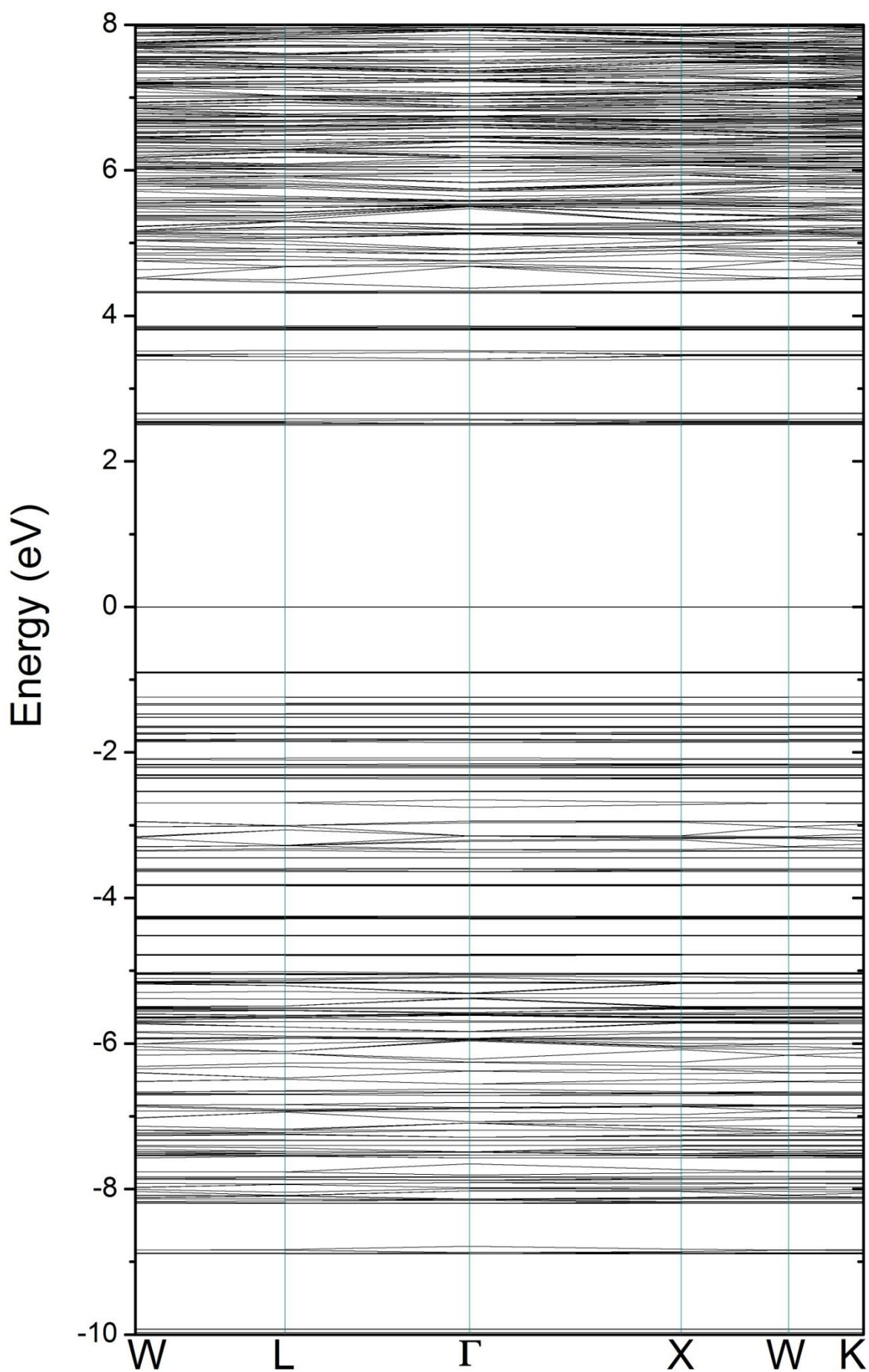


Figure S15. The electronic band structure of Cd-IRMOF-14. The Fermi level is set to zero and placed in the valence band maximum.

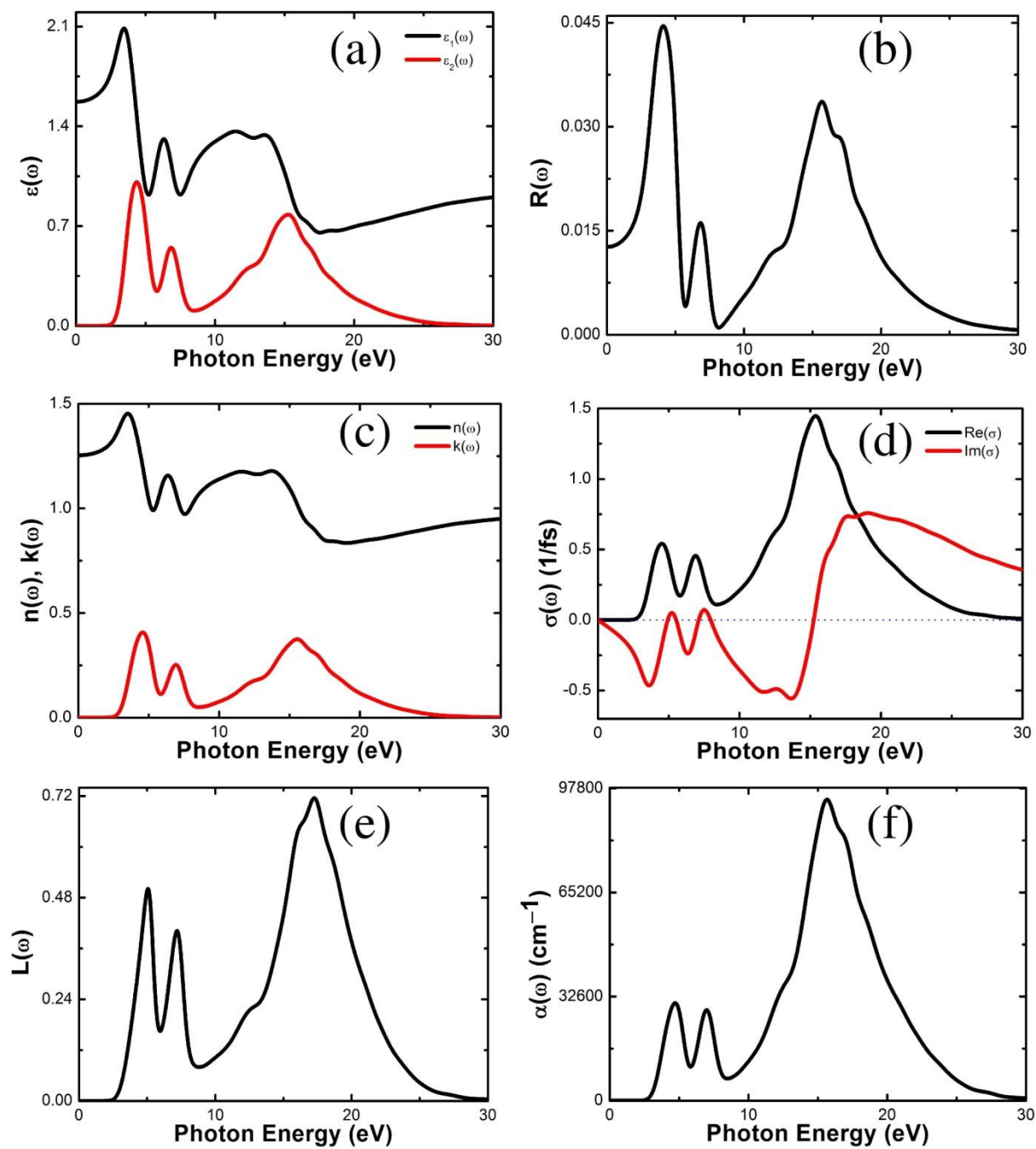


Figure S16. Calculated optical properties for Be-IRMOF-14: (a) dielectric function $\epsilon(\omega)$, (b) reflectivity $R(\omega)$, (c) refractive index $n(\omega)$; extinction coefficient $k(\omega)$, (d) optical conductivity $\sigma(\omega)$, (e) energy loss function $L(\omega)$, (f) absorption $\alpha(\omega)$.

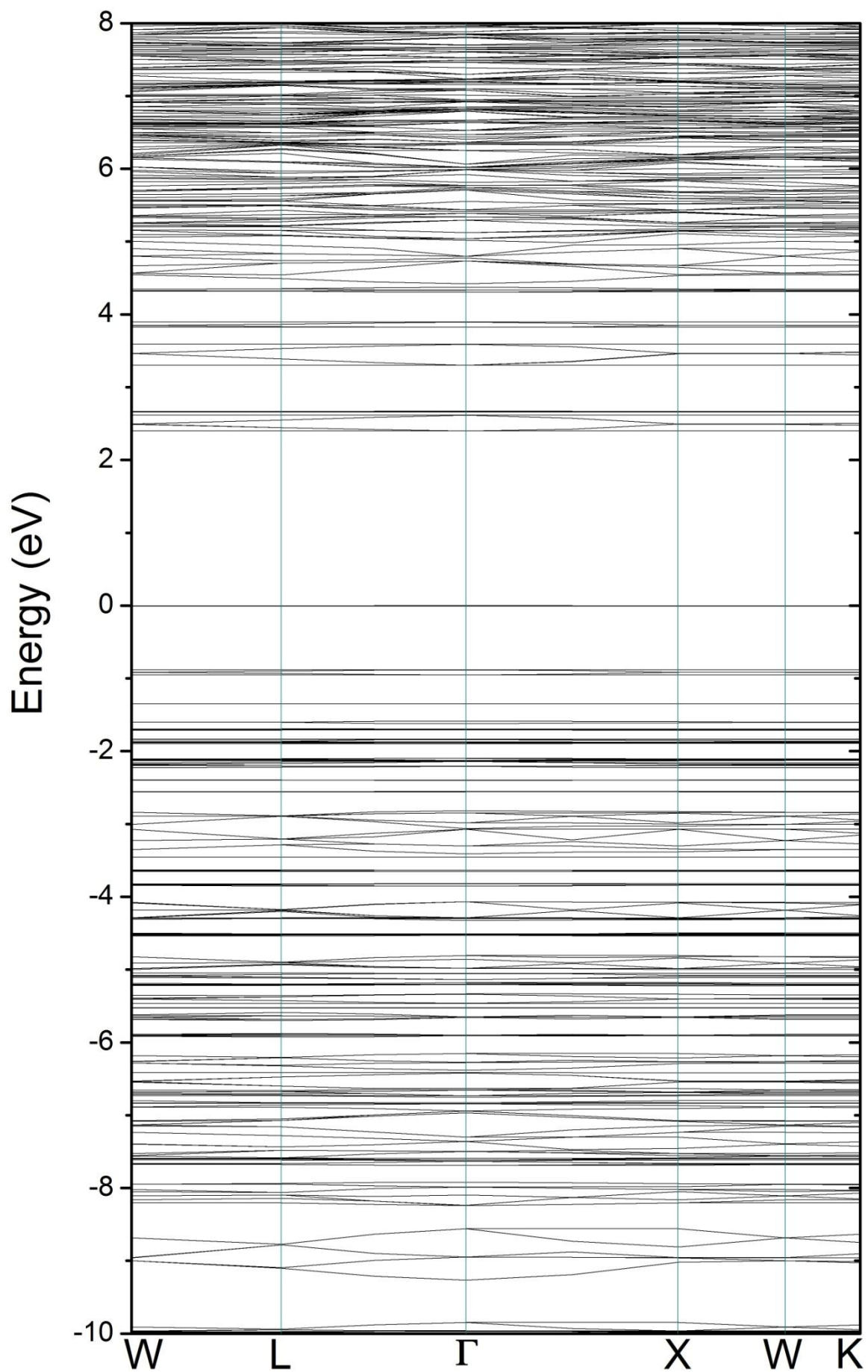


Figure S17. The electronic band structure of Be-IRMOF-14. The Fermi level is set to zero and placed in the valence band maximum.

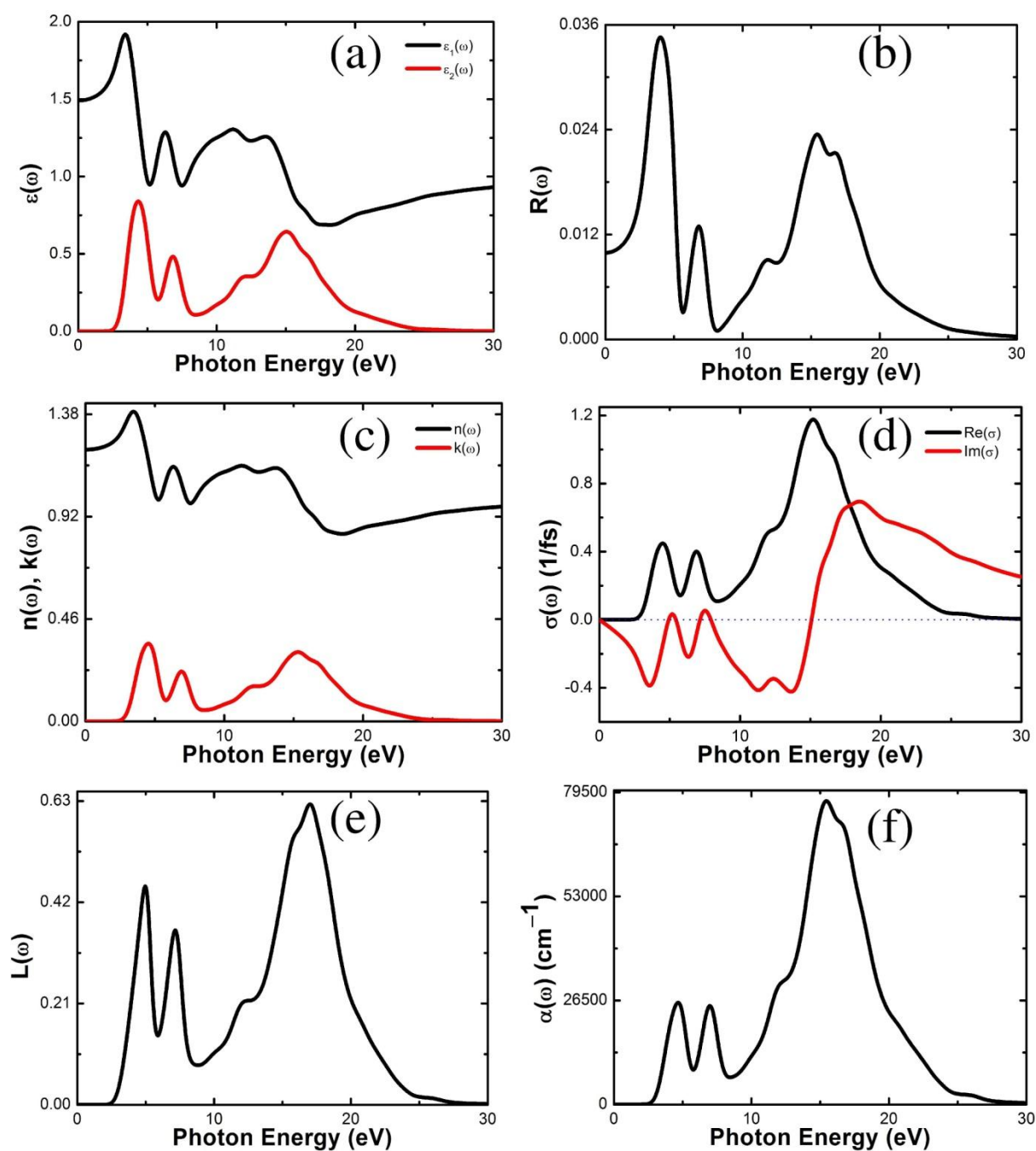


Figure S18. Calculated optical properties for Mg-IRMOF-14: (a) dielectric function $\epsilon(\omega)$, (b) reflectivity $R(\omega)$, (c) refractive index $n(\omega)$; extinction coefficient $k(\omega)$, (d) optical conductivity $\sigma(\omega)$, (e) energy loss function $L(\omega)$, (f) absorption $\alpha(\omega)$.

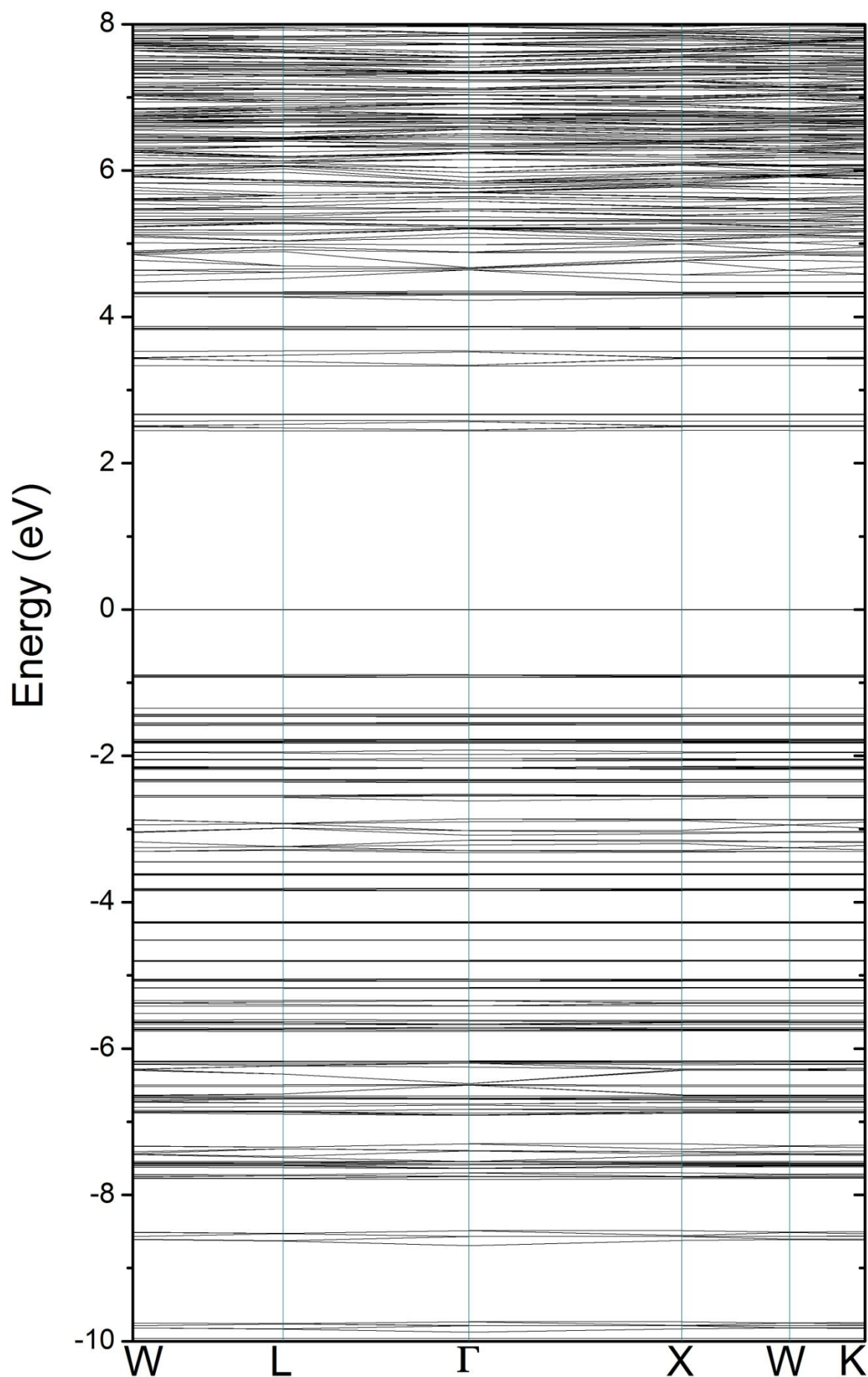


Figure S19. The electronic band structure of Mg-IRMOF-14. The Fermi level is set to zero and placed in the valence band maximum.

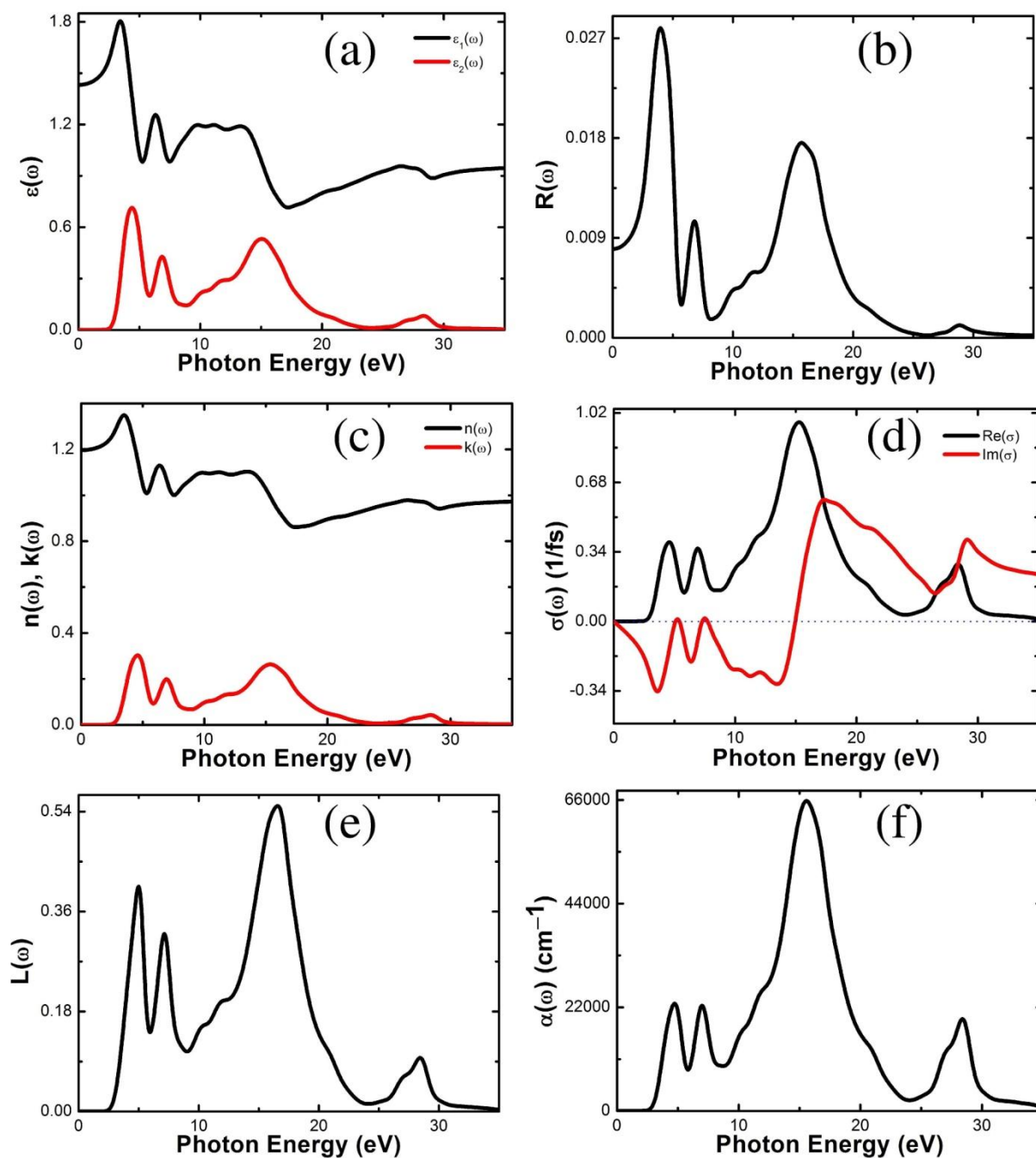


Figure S20. Calculated optical properties for Ca-IRMOF-14: (a) dielectric function $\epsilon(\omega)$, (b) reflectivity $R(\omega)$, (c) refractive index $n(\omega)$; extinction coefficient $k(\omega)$, (d) optical conductivity $\sigma(\omega)$, (e) energy loss function $L(\omega)$, (f) absorption $\alpha(\omega)$.

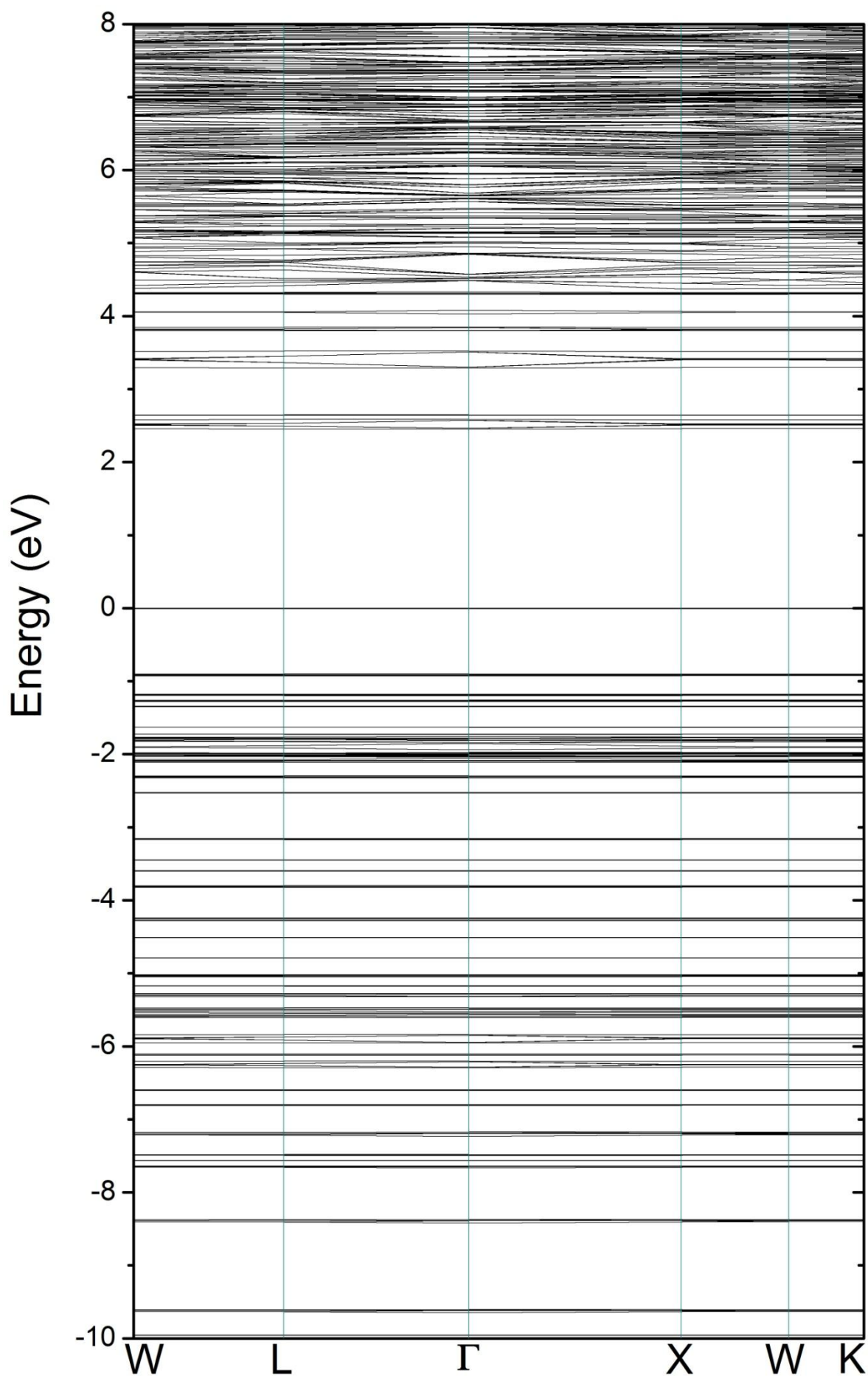


Figure S21. The electronic band structure of Ca-IRMOF-14. The Fermi level is set to zero and placed in the valence band maximum.

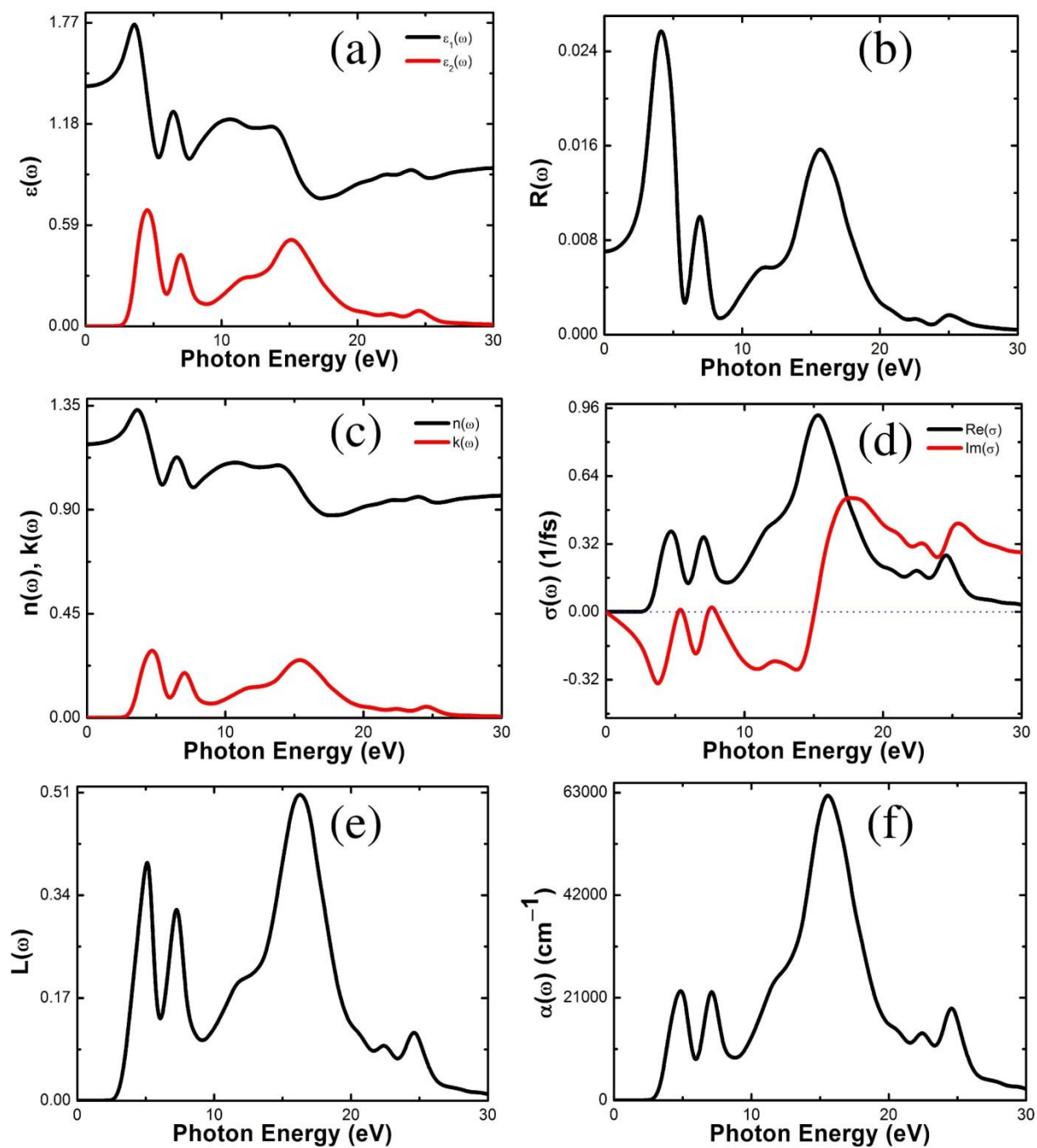


Figure S22. Calculated optical properties for Sr-IRMOF-14: (a) dielectric function $\epsilon(\omega)$, (b) reflectivity $R(\omega)$, (c) refractive index $n(\omega)$; extinction coefficient $k(\omega)$, (d) optical conductivity $\sigma(\omega)$, (e) energy loss function $L(\omega)$, (f) absorption $\alpha(\omega)$.

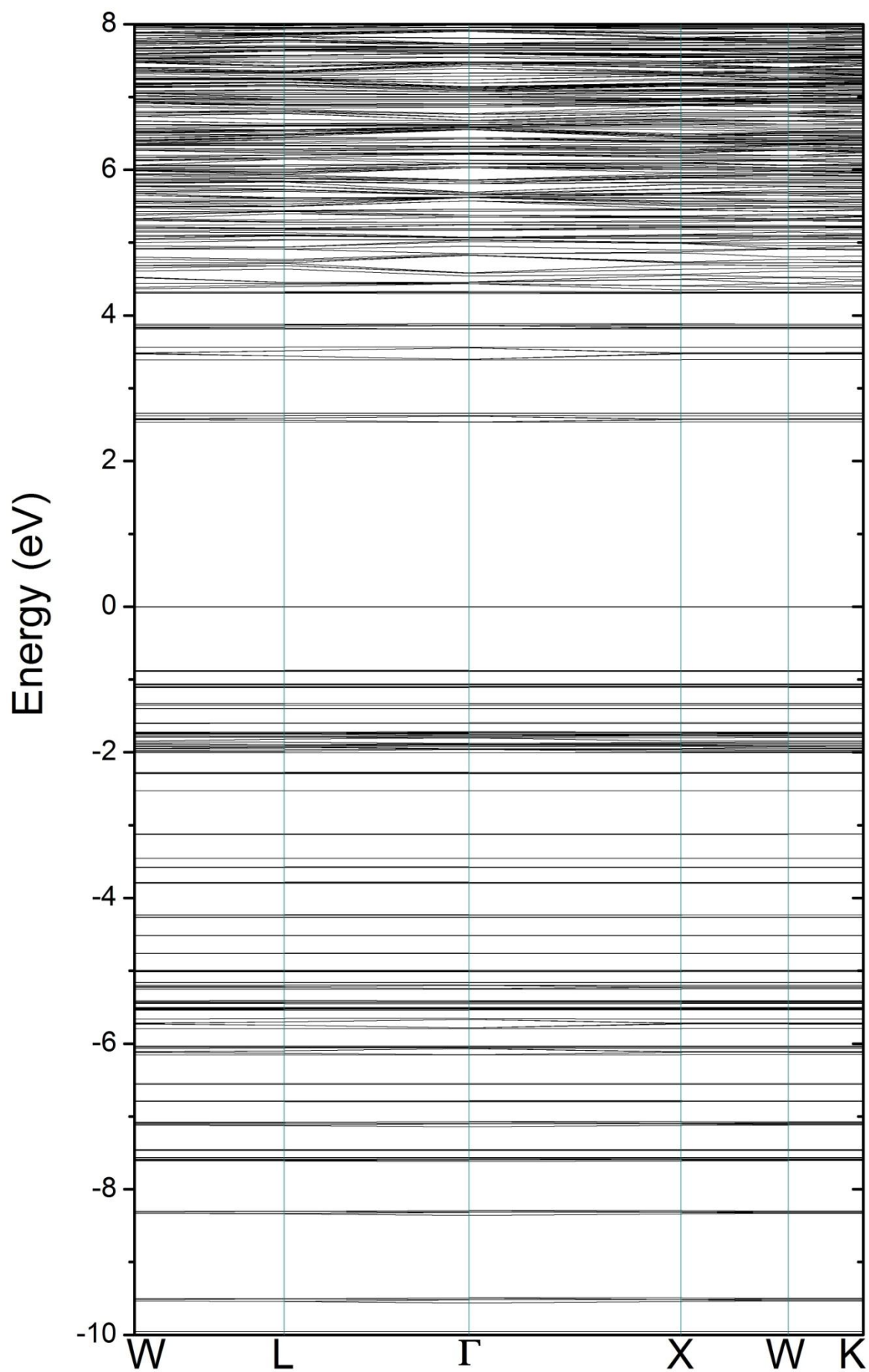


Figure S23. The electronic band structure of Sr-IRMOF-14. The Fermi level is set to zero and placed in the valence band maximum.

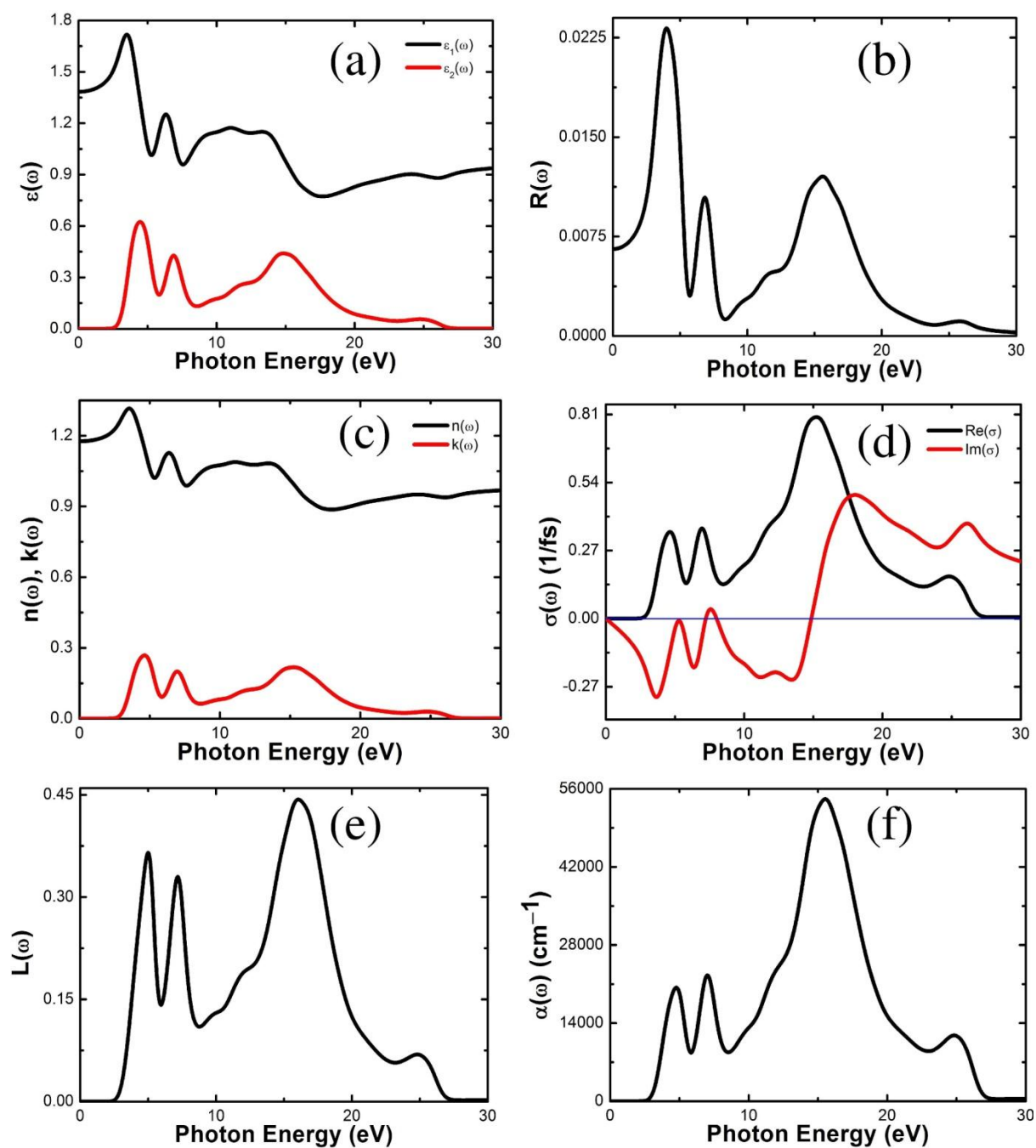


Figure S24. Calculated optical properties for Ba-IRMOF-14: (a) dielectric function $\epsilon(\omega)$, (b) reflectivity $R(\omega)$, (c) refractive index $n(\omega)$; extinction coefficient $k(\omega)$, (d) optical conductivity $\sigma(\omega)$, (e) energy loss function $L(\omega)$, (f) absorption $\alpha(\omega)$.

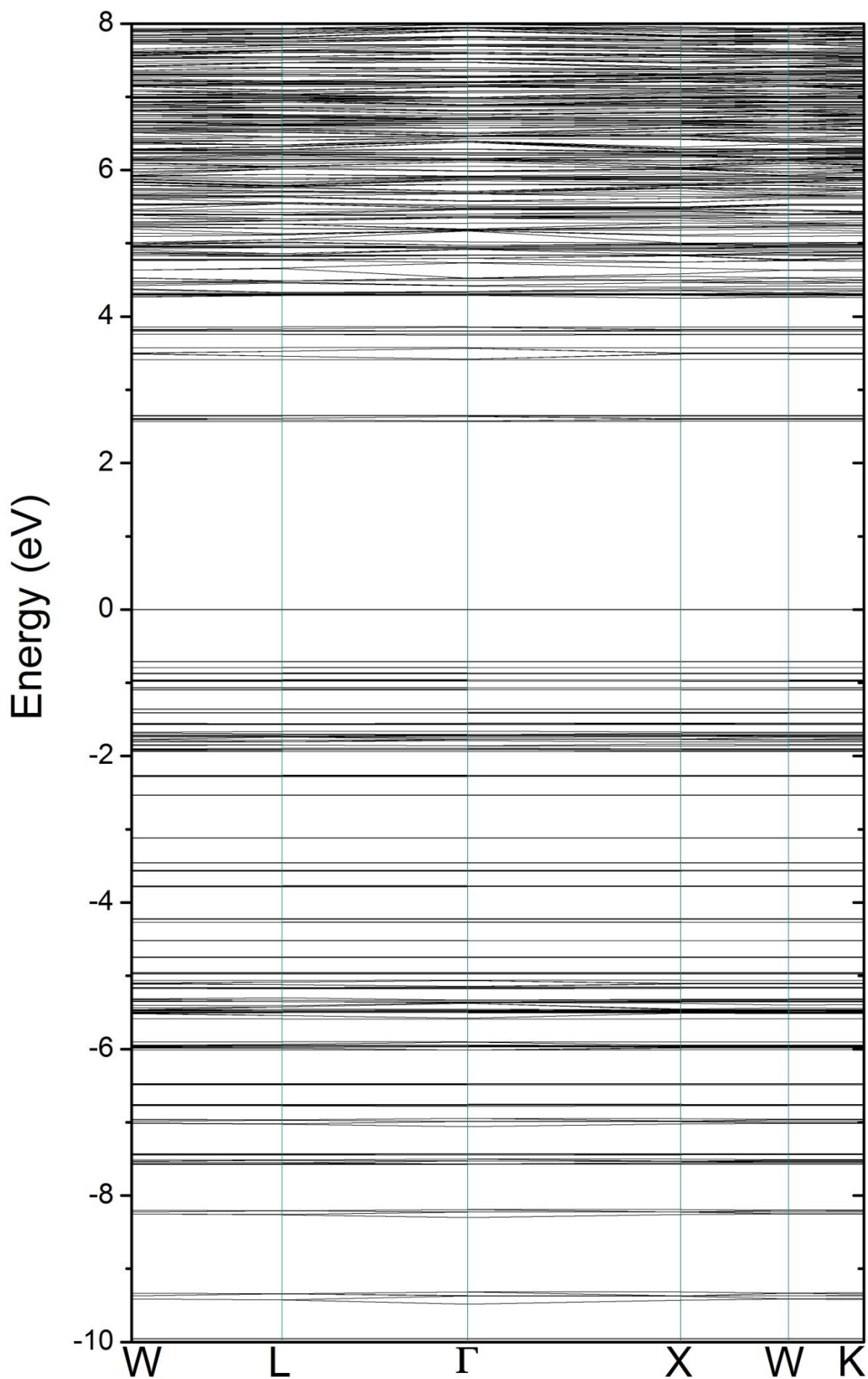


Figure S25. The electronic band structure of Ba-IRMOF-14. The Fermi level is set to zero and placed in the valence band maximum.

Table S1. Calculated Mulliken effective charges (MEC), bond overlap populations (BOP), and Bader charges (BC; given in terms of e) for M -IRMOF-14 ($M = \text{Zr, Cd, Be, Mg, Ca, Sr, Ba}$).^a

Material	Atom	MEC (e)	BOP	BC (e)	
IRMOF-14	Zn	+1.30	0.26-0.29 (Zn-O)	+1.3898	
	O1	-1.05	0.26 (O1-Zn)	-1.3341	
	O2	-0.65	0.29 (O2-Zn)	-1.7545	
	C1		-0.25	1.11 (C1-C2)	+0.0871
				1.10 (C1-C3)	
	C2		-0.01	1.06 (C2-C5)	-0.0174
				0.98 (C2-C6)	
	C3	-0.06	0.84 (C3-C4)	-0.0564	
	C4	+0.61	0.91 (C4-O2)	+2.6478	
	C5	0.00	1.09 (C5-C5)	-0.0507	
	C6	-0.28	1.21 (C6-C6)	+0.0249	
	H1	+0.27	0.90 (H1-C1)	+0.0348	
H2	+0.29	0.87 (H2-C6)	+0.0027		
Cd-IRMOF-14	Cd	+1.27	0.21-0.23 (Cd-O)	+1.3248	
	O1	-1.02	0.21 (O1-Cd)	-1.2151	
	O2	-0.65	0.23 (O2-Cd)	-1.7489	
	C1		-0.25	1.10 (C1-C2)	+0.0799
				1.10 (C1-C3)	
	C2		-0.01	1.06 (C2-C5)	-0.0038
				0.98 (C2-C6)	
	C3	-0.06	0.83 (C3-C4)	-0.0431	
	C4	+0.63	0.90 (C4-O2)	+2.6542	
	C5	0.00	1.09 (C5-C5)	-0.0404	
	C6	-0.28	1.21 (C6-C6)	-0.0046	
	H1	+0.27	0.89 (H1-C1)	+0.0228	
H2	+0.29	0.87 (H2-C6)	+0.0288		
Be-IRMOF-14	Be	+1.14	0.36-0.37 (Be-O)	+2.0000	
	O1	-0.96	0.37 (O1-Be)	-2.0012	
	O2	-0.63	0.36 (O2-Be)	-1.9093	
	C1		-0.26	1.10 (C1-C2)	+0.0720
				1.09 (C1-C3)	
	C2		-0.01	1.06 (C2-C5)	+0.0046
				0.98 (C2-C6)	
	C3	-0.05	0.85 (C3-C4)	-0.0635	
	C4	+0.61	0.92 (C4-O2)	+2.6509	
	C5	+0.01	1.09 (C5-C5)	-0.0501	
	C6	-0.28	1.21 (C6-C6)	+0.0166	
	H1	+0.30	0.87 (H1-C1)	+0.0400	
H2	+0.30	0.87 (H2-C6)	+0.0077		
Mg-IRMOF-14	Mg	+1.59	0.23 (Mg-O)	+2.0000	
	O1	-1.29	0.23 (O1-Mg)	-1.9977	
	O2	-0.71	0.23 (O2-Mg)	-1.9009	
	C1		-0.25	1.11 (C1-C2)	+0.0432
				1.10 (C1-C3)	
	C2		-0.01	1.06 (C2-C5)	-0.0446
				0.98 (C2-C6)	
	C3	-0.07	0.85 (C3-C4)	-0.0203	
	C4	+0.60	0.91 (C4-O2)	+2.6735	
C5	0.00	1.09 (C5-C5)	+0.0247		

	C6	-0.28	1.21 (C6-C6)	-0.0312
	H1	+0.27	0.90 (H1-C1)	+0.0558
	H2	+0.29	0.87 (H2-C6)	+0.0385
Ca-IRMOF-14	Ca	+1.35	0.14-0.18 (Ca-O)	+1.6188
	O1	-1.15	0.18 (O1-Ca)	-1.4955
	O2	-0.70	0.14 (O2-Ca)	-1.8283
	C1	-0.26	1.10 (C1-C2)	-0.0003
			1.09 (C1-C3)	
	C2	-0.01	1.06 (C2-C5)	-0.0057
			0.98 (C2-C6)	
	C3	-0.06	0.82 (C3-C4)	+0.0032
	C4	+0.66	0.89 (C4-O2)	+2.7311
	C5	0.00	1.09 (C5-C5)	-0.0182
	C6	-0.28	1.21 (C6-C6)	+0.0035
	H1	+0.30	0.87 (H1-C1)	+0.0411
H2	+0.29	0.87 (H2-C6)	+0.0167	
Sr-IRMOF-14	Sr	+1.39	0.14-0.17 (Sr-O)	+1.6118
	O1	-1.14	0.17 (O1-Sr)	-1.4597
	O2	-0.70	0.14 (O2-Sr)	-1.8202
	C1	-0.26	1.10 (C1-C2)	+0.0615
			1.09 (C1-C3)	
	C2	-0.01	1.06 (C2-C5)	+0.0098
			0.98 (C2-C6)	
	C3	-0.06	0.82 (C3-C4)	-0.0730
	C4	+0.64	0.89 (C4-O2)	+2.6979
	C5	0.00	1.09 (C5-C5)	-0.0578
	C6	-0.28	1.21 (C6-C6)	+0.0165
	H1	+0.30	0.87 (H1-C1)	+0.0303
H2	+0.29	0.87 (H2-C6)	+0.0031	
Ba-IRMOF-14	Ba	+1.37	0.11-0.16 (Ba-O)	+1.6127
	O1	-1.08	0.16 (O1-Ba)	-1.4214
	O2	-0.69	0.11 (O2-Ba)	-1.8273
	C1	-0.26	1.10 (C1-C2)	+0.0697
			1.09 (C1-C3)	
	C2	-0.01	1.06 (C2-C5)	-0.0109
			0.98 (C2-C6)	
	C3	-0.06	0.81 (C3-C4)	-0.0702
	C4	+0.64	0.89 (C4-O2)	+2.7244
	C5	0.00	1.09 (C5-C5)	-0.0535
	C6	-0.28	1.21 (C6-C6)	+0.0210
	H1	+0.29	0.87 (H1-C1)	+0.0294
H2	+0.29	0.87 (H2-C6)	-0.0013	

^a The atoms are numbered according to Fig. 1 and the partial density of states (PDOS) in Fig. 3 in the electronic structure section of the manuscript.